Environmental Science and Pollution Research (2021) 28:24847–24871
https://doi.org/10.1007/s11356-021-13008-3

REVIEW ARTICLE

Catalytic oxidation of CO on noble metal-based catalysts

Chenglin Feng[1,2] · Xiaolong Liu[2] · Tingyu Zhu[2,3] · Mengkui Tian[1]

Received: 16 November 2020 / Accepted: 12 February 2021 / Published online: 24 March 2021

Abstract

Carbon monoxide (CO) catalytic oxidation has gained increasing interest in recent years due to its application prospects. The noble metal catalysts commonly exhibit outstanding CO catalytic oxidation activity. Therefore, this article reviewed the recent research on the application of noble metal catalysts in the catalytic oxidation of CO. The effects of catalyst support, dopant, and physicochemical properties on the catalytic activity for CO oxidation are summarized. The influence of the presence of water vapor and sulfur dioxide in the reaction atmosphere on the catalytic activity in CO oxidation is emphatically discussed. Moreover, this paper discussed several reaction mechanisms of CO catalytic oxidation on noble metal catalysts. Finally, the challenges of removing CO by catalytic oxidation in practical industrial flue gas are proposed.

Keywords CO · Catalytic oxidation · Noble metal · Reaction mechanism

Introduction

CO is a colorless, odorless, and asphyxiating gas, which can lead to human poisoning when the CO content in the air is higher than 0.1% (Xu et al. 2020). CO is mainly emitted from industrial flue gas and motor vehicle exhaust, caused by incomplete combustion of fossil fuels. For example, the flue gas generated in the iron ore sintering process contains approximately 1% CO (Taira et al. 2016). Nowadays there is no effective treatment strategy for CO purification from industrial flue gas. The treatment method of CO in the exhaust gas of diesel vehicles is generally through catalytic oxidation CO using the three-way catalyst. The reaction process is shown in Eq. 1. Currently, catalytic oxidation of CO is recognized as the most energy-saving and efficient method for CO purification. Furthermore, as a typical gas-solid heterogeneous reaction, catalytic oxidation of CO is regarded as an extremely important topic for fundamental research. CO can be used as a probe molecule to investigate the catalyst structure, adsorption/desorption behavior, metal-support interaction, and catalytic reaction mechanism (Zhou et al. 2015).

$$CO + {}^{1}/_{2}O_2 \rightarrow CO_2 \quad (1)$$

In the past decades, numerous noble metal-based catalysts have been developed for CO oxidation, showing apparently higher catalytic activity than transition metal oxides (Prasad and Singh 2012). Bulk Au is inert to the catalytic oxidation of CO. Supported gold nanoparticles (NPs) catalysts have attracted widespread attention in recent years due to their excellent low-temperature CO oxidation activity, even catalytically oxidizing CO at − 70 °C (Haruta et al. 1987; Haruta 2011). CO is excessively adsorbed on the noble metal Pd and Pt sites, making O_2 unable to be adsorbed and activated, thereby inhibiting the catalytic activity of Pt- and Pd-based catalysts for CO oxidation under low-temperature conditions (<100 °C). However, when the temperature is improved, Pt- and Pd-based catalysts commonly show outstanding CO oxidation performance. Therefore, Pt and Pd are widely used in the CO purification of diesel vehicle exhaust as the active

Responsible Editor: Santiago V. Luis

✉ Xiaolong Liu
liuxl@ipe.ac.cn

✉ Tingyu Zhu
tyzhu@ipe.ac.cn

[1] School of Chemistry and Chemical Engineering, Guizhou University, Guiyang 550025, Guizhou, China

[2] Beijing Engineering Research Center of Process Pollution Control, National Engineering Laboratory for Hydrometallurgical Cleaner Production Technology, Institute of Process Engineering, Innovation Academy for Green Manufacture, Chinese Academy of Sciences, Beijing 100190, China

[3] Center for Excellence in Regional Atmospheric Environment, Institute of Urban Environment, Chinese Academy of Sciences, Xiamen 361021, China

components of the three-way catalysts (Zhou et al. 2015). In addition, there are many reports on Ag-, Ru-, Ir-, and Rh-based catalysts for CO catalytic oxidation (Grabchenko et al. 2020; Panagiotopoulou and Verykios 2017; Zhang et al. 2019a, b; Zhang et al. 2015). Here in this paper, CO oxidation over noble metals (Pt, Au, Pd, Ag, Ru, Rh, Ir) catalysts are reviewed as shown in Fig. 1. The support and dopant optimizations for higher CO catalytic efficiency are introduced. The influence of the physicochemical properties of noble metal catalysts on CO catalytic activity is summarized. Besides, this article also discusses the CO catalytic performance in harsh reaction atmospheres. Many studies have speculated on the reaction mechanism of CO catalytic oxidation on noble metal catalysts through experiments and theoretical calculations. Hence, the reaction mechanisms of CO oxidation over noble metal catalysts were discussed.

Pt-based catalysts

Effect of catalyst support

Catalyst support plays a vital role in CO oxidation. Zheng et al. (2016) reported a $Pt/MgFe_2O_4$ catalyst with high CO oxidation performance at room temperature. It was found that the support $MgFe_2O_4$ had an inverse spinel structure and could provide uncoordinated lattice oxygen as active oxygen species for CO oxidation. Lee et al. (2018a, b) reported that Pt/CeO_2 catalysts with fewer surface defects were obtained by heat-treated CeO_2 at 800 °C, thereby weakening the interaction between the active species and the support, forming less Pt–O–Ce bonds and giving a higher dispersion of Pt species and better catalytic efficiency. Zhou et al. (2016) reported that the CO oxidation activity was significantly affected by different facets of support anatase-TiO_2. Among them, Pt/TiO_2-101 and Pt/TiO_2-100 gave stronger CO oxidation activity than Pt/TiO_2-001, owing to that Pt species was more stable and higher dispersion on the facet 101 and facet 110 than the facet 001. Wang et al. (2014) clarified that the morphology of WO_3 has a significant influence on the activity of Pt catalysts for CO oxidation. Compared with the nanoparticle WO_3 support, the nanolamella WO_3-supported Pt catalyst has higher CO oxidation activity due to the higher dispersion of Pt on the support and metal-support interaction to form more Pt^0 species, which is more beneficial for CO activation to participate in the reaction. Lou and Liu (2017) prepared monoatomic Pt catalysts with different supports (Pt/Fe_2O_3, Pt/ZnO, and $Pt/\gamma\text{-}Al_2O_3$) and reported that water could promote the catalytic oxidation of CO. All catalysts would significantly increase the catalytic activity of CO in present water or hydroxyl groups on the support, indicating that the CO oxidation activity has nothing to do with the type of support. After -OH groups were removed from the support by heat treatment at 300 °C, the Pt catalyst supported on the reducible carrier (Fe_2O_3) has the highest CO catalytic activity. An et al. (2013a, b) found that the CO oxidation activity of Pt/Oxides catalyst was much higher than pure Pt and supports (Co_3O_4, NiO, MnO_2, Fe_2O_3, CeO_2). The created interface between the metal and the support was a key factor for obtaining high CO oxidation activity, because the metal-support interface forms an active phase that is easy to provide lattice oxygen. For example, the CoO active phase was formed on the Pt/Co_3O_4 catalyst metal

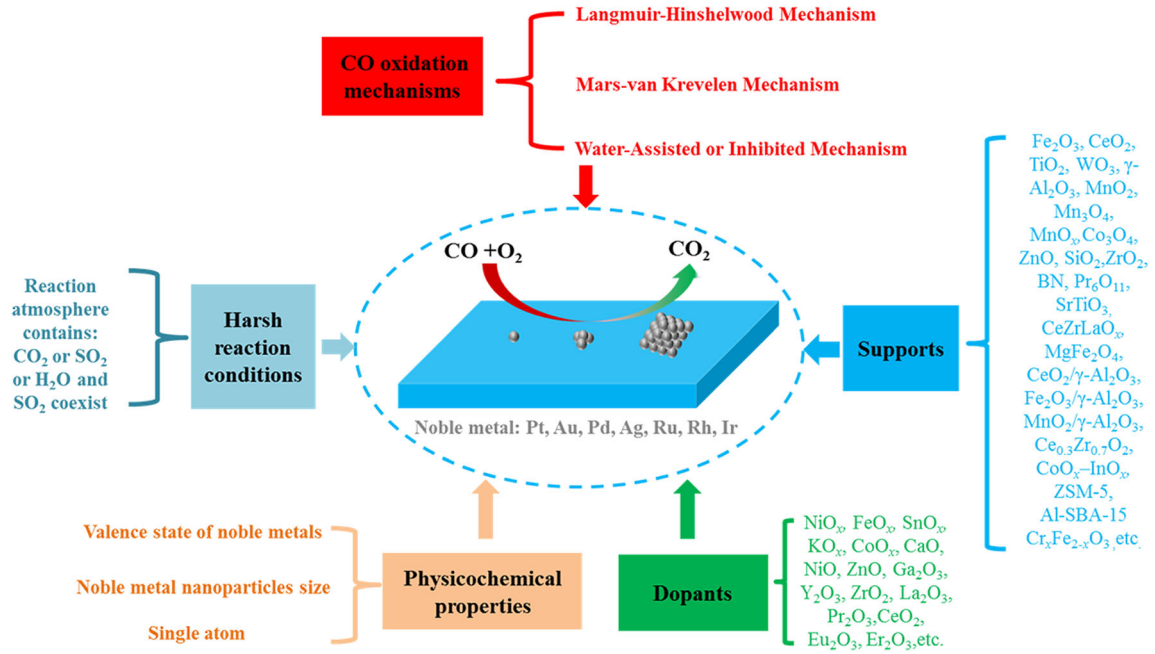

Fig. 1 Catalytic oxidation of CO on noble metal catalysts

interface. Zhang et al. (2019a, b) reported that novel β-MnO_2 support material in Pt/MnO_x catalyst greatly promoted CO oxidation. As a result, the CO oxidation activity of Pt/MnO_x catalyst at 100 °C was 5 times of the Pt/MnO_x-COM (COM, commercial) catalyst. Jung et al. (2014) prepared Pt/SiO_2 using the ultrasonic spray pyrolysis (USP) method for CO catalytic oxidation. The loading of Pt and the calcination temperature were systematically investigated. Among the catalysts, 4 wt% Pt/SiO_2 calcined at 600 °C contributed the highest CO catalytic activity.

Effect of dopant

Doping platinum-based catalysts is a common method to improve catalytic activity of CO. Cai et al. (2018) prepared a monoatomic NiO_x-coated nanoparticle Pt with a shell-core structure NiO_x/Pt/Al_2O_3 catalyst. The Pt/Al_2O_3 catalyst doped with NiO_x could produce a highly active metal oxide interface, thereby improving the catalytic activity. Meanwhile, the doping of NiO_x could improve the sintering resistance of Pt/Al_2O_3. Tomita et al. (2013) reported that Fe-doped Pt/γ-Al_2O_3 catalyst was used for CO removal in H_2-rich atmosphere at low temperature. Doping Fe increased the CO oxidation activity and selectivity of Pt/γ-Al_2O_3 catalyst, which was attributed to the formation of boundaries between Pt nanoparticles and FeO_x species, which led to the rapid reaction of CO adsorbed on Pt nanoparticles with oxygen species provided by the $Fe^{2+}\leftrightarrow Fe^{3+}$ redox cycle. Tanaka et al. (2015) also reported that FeO_x/Pt/TiO_2 catalyst doped with Fe at room temperature greatly promoted CO preferential oxidation and selectivity in the presence of water in the atmosphere. This was attributed to the dissociation of H_2O into H^+ and OH^- on FeO_x sites, where OH^- provided active oxygen species for CO oxidation. Margitfalvi and Irina (2002) doped Sn on Pt/SiO_2 catalyst to improve CO oxidation performance at low temperature. When Sn/Pt = (0.2–0.4), the catalyst contributed the highest CO oxidation activity, owing to the formation of high mobile Sn^{n+}-Pt ensemble sites at the bimetallic interface. Besides, CO oxidation activity of the catalyst decreased when stable SnO_x surface species were formed on the catalyst surface. Liu et al. (2015) improved the CO oxidation activity of Pt/Al_2O_3 catalyst by doping K. Doping K reduced the reaction energy barrier of the catalyst and improved the CO reaction order. In situ FTIR results showed that the CO adsorption peak on the 0.42K-2.0Pt/Al_2O_3 catalyst completely disappeared, while the CO adsorption peak still existed on the 2.0Pt/Al_2O_3 catalyst at 180 °C, indicating that K doping was beneficial for CO desorption and O_2 adsorption and activation. Zhao et al. (2018) introduced 1% Co ions into the Pt/TiO_2 catalyst using one-step flame spray pyrolysis process for CO oxidation. During the preparation process, Co^{2+} was oxidized to Co^{3+} ($Co^{2+}\rightarrow Co^{3+}+e^-$) to release electrons to the surface Pt species to suppress the sintering of Pt nanoparticles. In addition, in situ DRIFTS results showed that the introduction of Co ions was beneficial to desorption of CO adsorbed on Pt^0 sites.

Effect of physicochemical properties

The physicochemical properties of Pt-based catalysts are also important factors influencing CO oxidation activity, such as the particle size of Pt, dispersion, and platinum valence. As shown in Fig. 2, Kim et al. (2016) prepared Pt/TiO_2 catalysts treated with H_2 at different temperatures and found that the catalyst with high dispersion and small particle size of Pt species (Pt/TiO_2 (R)-600) gave higher catalytic activity at room temperature. Additionally, CO was more easily activated on Pt^0 than on Pt^{2+} sites. As a consequence, higher $Pt_{metallic}/Pt_{total}$ value gave higher CO oxidation activity of the catalyst. Besides, Liu et al. (2018a, b) prepared a brookite-TiO_2-supported Pt catalyst and found that under the same Pt loading, higher Pt^0 specific and dispersion of Pt nanoparticles would enhance the CO oxidation activity. In situ FTIR results showed that CO adsorbed on Pt^0 sites was easier to desorb to participate in the reaction, while CO was strongly adsorbed on $Pt^{\delta+}$ and Pt^{2+} sites. For Pt/SiO_2 catalyst (Jung et al. 2014), according to the TEM images, the 4wt%Pt/SiO_2 catalyst calcined at 600 °C for 30 min has smaller Pt nanoparticles size and higher dispersion than the 4 wt% Pt/SiO_2 calcined at 750 °C for 2 h. Higher dispersion of Pt nanoparticles means more CO adsorption and activation sites, thus leading to higher CO catalytic performance. Besides, single-atom Pt catalysts also showed excellent CO oxidation activity. Single-atom Pt commonly existed in the form of high valence on the catalysts. The high activity of single-atom Pt catalysts was attributed to the partially vacant 5d orbitals of high valence Pt atoms, which was conducive to the adsorption and activation of CO (Qiao et al. 2011). Wang et al. (2020) reported that the CO oxidation activity of a single-atom Pt catalyst (0.2Pt/$Cr_{1.3}Fe_{0.7}O_3$) was much higher than that of nanoparticle Pt catalyst (2Pt/$Cr_{1.3}Fe_{0.7}O_3$) under wet conditions. This was due to the weaker adsorption of CO on 0.2Pt/$Cr_{1.3}Fe_{0.7}O_3$ and easier participation in the reaction.

Effect of harsh reaction conditions

The reaction atmosphere has a great effect on the performance of CO oxidation over Pt-based catalysts. For the Pt/$Cr_xFe_{2-x}O_3$ catalyst (Wang et al. 2019), when 10% CO_2 was introduced into the reaction atmosphere, CO_2 could compete with CO for adsorption sites and formed carbonate species covering on the catalyst surface, thereby inhibiting the CO oxidation activity. When 10% water vapor was introduced, the water vapor not only promoted the decomposition of carbonate species on the catalyst surface, but also accelerated the reaction of -OH groups on the catalyst carrier and CO due to the

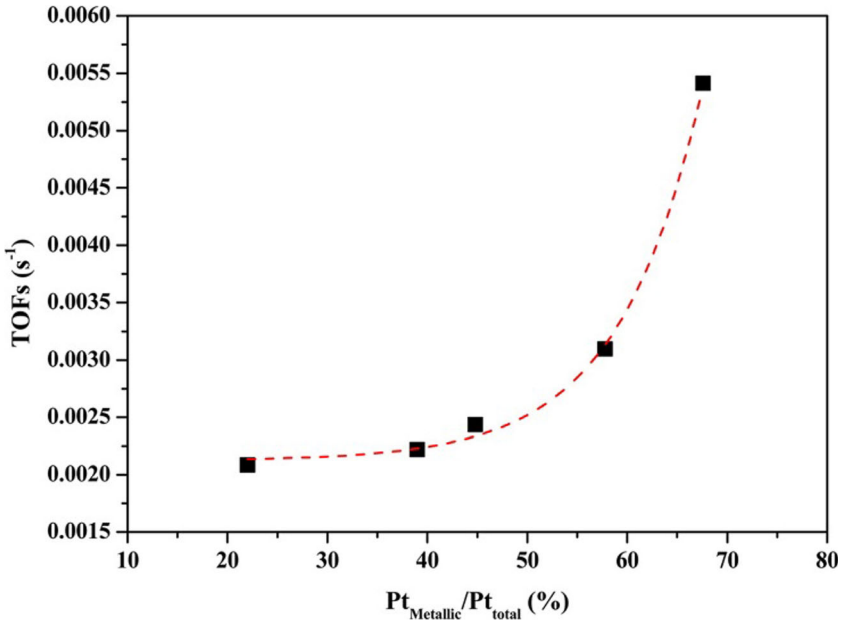

Fig. 2 Correlation between the $Pt_{metallic}/Pt_{total}$ ratio and the TOF of catalysts (Kim et al. 2016). Copyright 2016, American Chemical Society

dissociation of water vapor into -OH groups. It was reported that the presence of only SO_2 in the atmosphere also led to the sulfation of the support. The degree of sulfation of the support was related to the temperature and the type of carries. When the temperature was lower than 200 °C, SO_3^{2-} and SO_4^{2-} species coexisted on the support of Al_2O_3. When the temperature was higher than 300 °C, SO_4^{2-} species was predominant on Al_2O_3 (Smirnov et al. 2014). When the temperature was lower than 100 °C, the CeO_2 support was sulfided to $Ce(SO_4)_2$, resulting in serious deactivation of catalyst. It was also reported that when the temperature was lower than 200 °C, the active component Pt was vulcanized to PtS, and when the temperature is higher than 200 °C with oxygen, S^{2-} species was converted to SO_4^{2-} species and quickly migrated to the catalyst surface (Wakita et al. 2005). At present, it is generally accepted that Pt is not easily sulfated. As shown in Fig. 3, in the atmosphere where H_2O and SO_2 coexist, SO_2 was oxidized to form SO_3 on a Pt-based catalyst at temperature of 200–300 °C, and the generated SO_3 reacted with H_2O to form sulfuric acid (Taira et al. 2016). The sulfuric acid generated on the catalyst not only caused the catalyst to be desulfurized and deactivates the catalyst, but also did not reach the boiling point of sulfuric acid when the temperature was lower than 300 °C, which led to the active site covered by sulfuric acid. Taira and Einaga (2019) prepared Pt/TiO_2 catalysts with different pore sizes and found that the catalyst with greater pore size (>10 nm) had stronger anti-sulfur performance, owing to the generated sulfuric acid did not easily block the catalyst with larger pore size, and the reactive gases could contact with the Pt sites. However, the sulfuric acid adsorbed on the catalyst was removed by heat treatment at 300 °C, and the performance of CO oxidation was not completely recovered. The generated sulfuric acid caused the surface of TiO_2 support to be sulfated to form a layer of $TiOSO_4$ species. This layer of $TiOSO_4$ species inhibited the interaction between -OH groups on support and CO on Pt sites, resulting in a decrease in catalytic activity.

Reaction mechanisms

In recent years, the catalytic oxidation mechanism of CO on Pt/Oxides catalysts under dry reaction atmosphere ($CO + O_2$) has been extensively investigated. They are generally divided into two categories: typical Langmuir-Hinshelwood mechanism (L-H mechanism) and Mars-van Krevelen mechanism (MvK mechanism). Additionally, in the wet reaction atmosphere, water vapor seems to change the CO oxidation pathway over Pt/Oxides catalysts, which is marked as Water-Assisted Mechanism or Water-Inhibited Mechanism (Ishida et al. 2020).

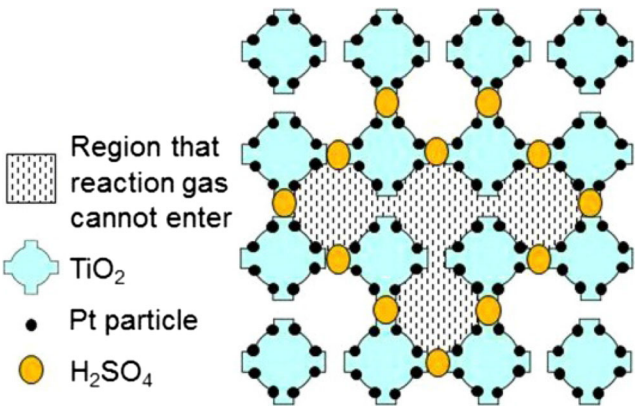

Fig. 3 Mechanism of sulfuric acid blocking catalyst pores (Taira et al. 2016). Copyright 2016, American Chemical Society

Langmuir-Hinshelwood mechanism

The pathway of CO oxidation over Pt-based catalyst with an inert support was generally considered to be the L-H Mechanism. As shown in Fig. 4, for the single-atom Pt/θ-Al_2O_3 (010) catalyst, density functional theory (DFT) calculations and experimental results proved that O_2 oxidizes the Pt atom and reacts with the adsorbed CO to form carbonate species. The carbonate species decomposes to release CO_2 and the oxygen atom adsorbed on the Pt atom. Then, the oxygen atom reacts with another CO to form CO_2 to complete the catalytic cycle (Moses-DeBusk et al. 2013). As shown in Fig. 5, Ganzler et al. (2019) revealed the oxidation mechanism of CO over Pt/CeO_2 and Pt/Al_2O_3 catalysts by Spatially Resolved Structure-Activity Correlations. At low temperatures, the activity of the Pt/CeO_2 catalyst was higher than the Pt/Al_2O_3 catalyst due to its more active oxygen species at the Pt-CeO_2 interface. The low activity of the Pt/Al_2O_3 catalyst at low temperature was attributed to the excessive adsorption of CO on the Pt nanoparticles, indicating that O_2 could not be adsorbed, which inhibited the L-H reaction pathway. Under high-temperature conditions, the weakening of CO adsorption on Pt/CeO_2 catalyst and Pt/Al_2O_3 catalyst led to easy adsorption and activation of O_2 at Pt sites. Meanwhile, the catalytic oxidation of CO over Pt/CeO_2 and Pt/Al_2O_3 followed the L-H mechanism. The Pt-CeO_2 interface still adsorbed and activated O to provide active oxygen species for CO oxidation. Besides, the intermediate products produced by CO through the L-H reaction

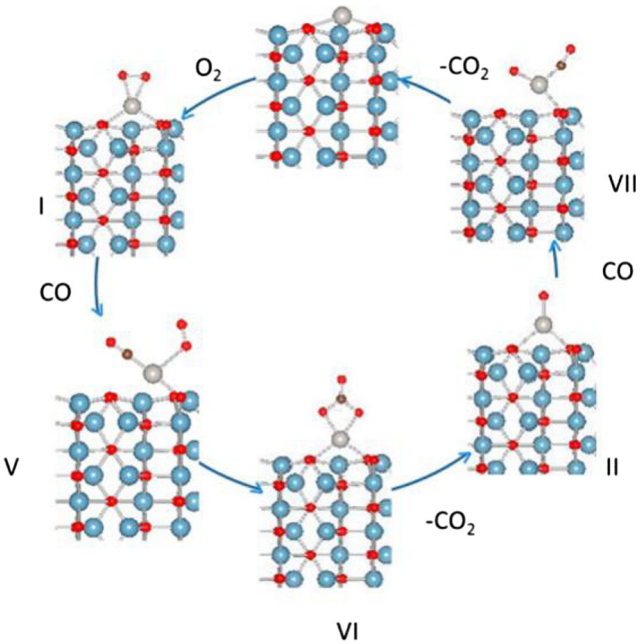

Fig. 4 Pathway for CO oxidation on single Pt atoms supported on the (010) surface of θ-Al_2O_3 (Moses-DeBusk et al. 2013). Copyright 2013, American Chemical Society

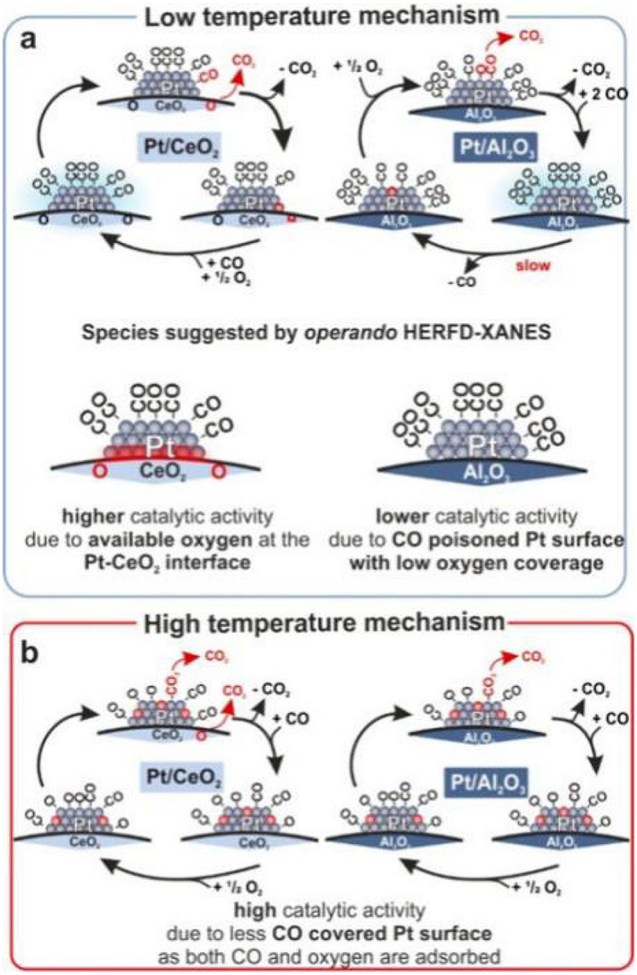

Fig. 5 Low-temperature and high-temperature CO oxidation mechanism on Pt/CeO_2 and Pt/Al_2O_3 catalysts (Ganzler et al. 2019). Copyright 2019, American Chemical Society

pathway were still controversial. Allian et al. (2011) believed that the formation of O-O-C=O species by CO and O_2 chemically adsorbed on Pt clusters was a thermodynamically more feasible intermediate product. Because this CO-assisted O_2 dissociation pathway avoided the high energy barrier required for O_2 dissociation due to excessive CO adsorption. O-O-C=O species then decompose into CO_2 and chemisorbed oxygen atoms. The chemically adsorbed oxygen atom then reacts with CO to form CO_2 completing the catalytic cycle. CO oxidation via CO*-Assisted O_2 Dissociation Route was as follows:

$$CO + {}^{*}\blacksquare \leftrightarrow CO^{*} \quad (2)$$

$$O_2 + {}^{*}\blacksquare \leftrightarrow O_2^{*} \quad (3)$$

$$O_2^{*} + CO^{*} \rightarrow CO_2^{*} + O^{*} \quad (4)$$

$$O^{*} + CO^{*} \rightarrow {}^{*}\blacksquare + CO_2^{*} \quad (5)$$

$$CO_2^{*} \rightarrow {}^{*}\blacksquare + CO_2 \quad (6)$$

* is the adsorption site.

In addition, there were also reported that the chemically adsorbed O_2 dissociates into oxygen atoms and then reacted with the chemically adsorbed CO to product CO_2 (Bourane 2004), as shown in Eqs. 7–10.

$$CO_{gas} \leftrightarrow CO_{ads} \quad (7)$$

$$O_{2gas} \leftrightarrow 2O_{ads} \quad (8)$$

$$CO_{ads} + O_{ads} \rightarrow CO_{2ads} \quad (9)$$

$$CO_{2ads} \rightarrow CO_{2gas} \quad (10)$$

Mars-van Krevelen mechanism

The pathway of CO oxidation over Pt-based catalyst with a strong oxygen storage capacity support was generally considered to be the MvK Mechanism. CO is chemically adsorbed on the Pt site and reacts with the lattice oxygen on the support to generate CO_2. The support was partially reduced due to the formation of oxygen vacancies. The O_2 molecules in the gas phase replenish the lattice oxygen to complete the catalytic cycle. This pathway avoids the competitive adsorption of CO and O_2 at low temperatures. As illustrated in Fig. 6, on the $Pt/MgFe_2O_4$ catalyst, the CO catalytic oxidation mechanism proposed by Zheng et al. (2016) followed the MvK Mechanism at room temperature. On the $Pt/Cr_xFe_{2-x}O_3$ catalyst, Wang et al. (2019) believed that the catalytic oxidation reaction of CO under the dry condition followed the MvK mechanism and proposed the elementary reaction through

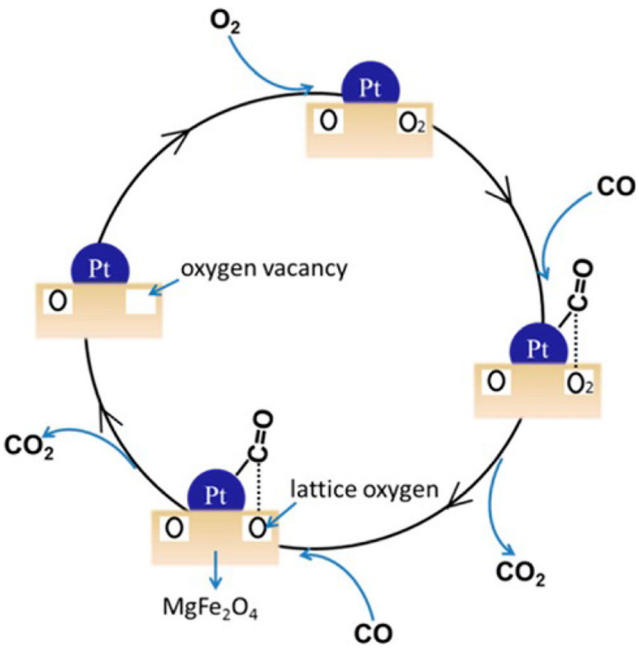

Fig. 6 Proposed CO oxidation mechanism on $Pt/MgFe_2O_4$ catalyst (Zheng et al. 2016). Copyright 2016, American Chemical Society

kinetic calculations, as shown in Eqs. 11–14. Moreover, On the Pt/Oxides catalyst, the CO chemically adsorbed on the Pt sites migrates to the metal-support interface and reacts with the lattice oxygen of the active phase at the metal interface to generate CO_2 and form oxygen vacancies. The reduced carrier is oxidized by gas-phase oxygen to complete the catalytic process (An et al. 2013a, b).

$$2\left[CO + Pt^{*} \leftrightarrow CO{-}Pt\right] \quad (11)$$

$$2[CO{-}Pt + M{-}[O] \rightarrow CO_2{-}Pt + M{-}[\blacksquare]\,] \quad (12)$$

$$2\left[CO_2{-}Pt \leftrightarrow CO_2 + Pt^{*}\,\right] \quad (13)$$

$$O_2 + 2\,M{-}[\blacksquare] \rightarrow 2\,M{-}[O] \quad (14)$$

Pt^{*} refers to the active site on Pt. $M-[O]$ refers to the lattice oxygen on the support. $M-[\blacksquare]$ refers to oxygen vacancy on the support.

Water-Assisted Mechanism

It has been reported that in Pt/TiO_2, the -OH groups on the catalyst support could react with CO. Therefore, the -OH groups on the support plays an important role in the catalytic oxidation of CO. Many literatures reported the phenomenon that water vapor promoted the catalytic oxidation of CO on Pt-based catalysts and proposed the reaction mechanism of water vapor to promote the catalytic oxidation of CO. Wang et al. (2016) clarified that water vapor considerably promoted the catalytic oxidation of CO over single-atom Pt_1/CeO_2. Isotope-labeling experiments revealed that $CO^{18}O$ accounts for half of the total CO_2 when the reaction temperature was higher than 90 °C. Therefore, the results strongly proved that when water vapor existed in the reaction atmosphere on the single-atom Pt_1/CeO_2 catalyst, water vapor could directly participate in the catalytic oxidation reaction of CO. Furthermore, on the single-atom Pt_1/CeO_2 catalyst, the Water-Mediated Mars-van Krevelen Mechanism in which H_2O directly participated in the catalytic oxidation of CO was proposed by DFT calculations (Fig. 7). The specific reaction pathway is as follows: (1) Water molecules are adsorbed on the CeO_2 support and dissociated into -OH bonded to Ce atoms, -H radicals bonded with adjacent lattice oxygen form lattice hydroxyl groups. (2) CO adsorbed on the Pt atomic site quickly reacts with -OH on the Ce atom to form intermediate product -COOH species. (3) -COOH species reacts with the lattice hydroxyl group to form CO_2 and H_2O, and the support is partially reduced due to the formation of oxygen vacancies. (4) O_2 in the gas-phase supplements lattice oxygen. For $Pt/Cr_{1.3}Fe_{0.7}O_3$ catalyst (Wang et al. 2019), the CO catalytic performance at 80 °C was promoted when 10% water vapor was introduced. According to the XPS O 1s characterization, it was found that the proportion of -OH groups on the surface of the catalyst after steam

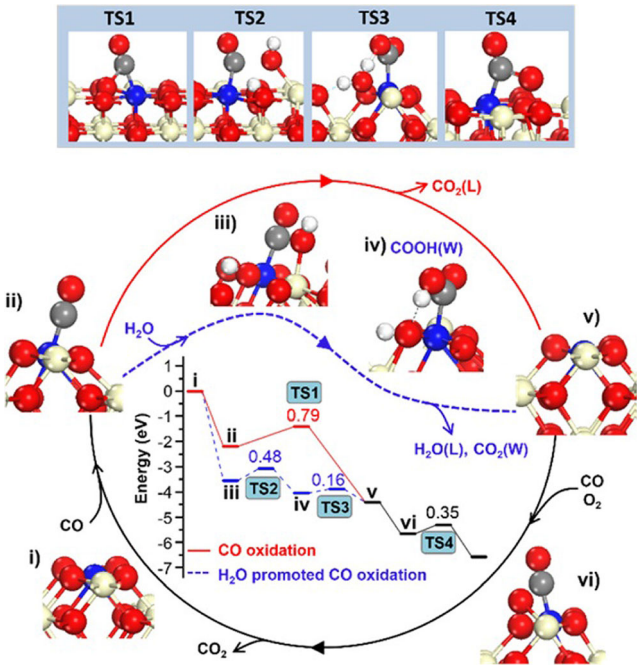

Fig. 7 Proposed reaction pathways for CO direct oxidation and H_2O-promoted CO oxidation on Pt_1/CeO_2 (110) (Wang et al. 2016). Copyright 2016, American Chemical Society

treatment was 29.2%, indicating that the dissociation of water vapor on the catalyst surface might be the reason for increasing of hydroxyl groups. Moreover, on the $2Pt/Cr_{1.3}Fe_{0.7}O_3$ and $0.2Pt/Cr_{1.3}Fe_{0.7}O_3$ catalyst (Wang et al. 2020), in situ FTIR results found that without water vapor in the reaction atmosphere, the hydroxyl groups (3728 cm^{-1} and 3693 cm^{-1}) on the catalyst gradually decreased, and the formate species (1600 cm^{-1}) and other carbonate species gradually increased. When 10% water vapor was introduced into the reaction atmosphere, the hydroxyl species and formate species on the surface of the catalyst increase significantly. The increase of formate species might be caused by the reaction of surface hydroxyl with CO. When water vapor was taken out of the reaction atmosphere, the hydroxyl groups on the surface of the catalyst dropped sharply. These results indicated that the way of water vapor promoted the catalytic oxidation of CO over the $2Pt/Cr_{1.3}Fe_{0.7}O_3$ is that the hydroxyl groups generated from the dissociation of water vapor continuously react with the CO adsorbed on the Pt sites. As illustrated in Fig. 8 and Eqs. 15–20, the reaction mechanism of water vapor promoted CO oxidation on the $Pt/Cr_{1.3}Fe_{0.7}O_3$ catalyst was proposed according to the kinetic calculations. The specific reaction pathway is as follows: (1) CO chemical adsorbs on the Pt sites. (2) Hydrolysis dissociates into -OH species. (3) -OH species reacts with CO at the interface to form -COOH species, and -COOH species decomposes into CO_2 and -H radicals. (4) -H radicals react with -OH to generate H_2O. (5) Gas-phase O_2 supplements oxygen vacancies to complete the catalytic cycle. Besides, some reports revealed that water molecules on Pt-based catalysts promote the catalytic oxidation of CO through promoting the activation of O_2. Liu et al. (2018a, b) calculated from DFT and found that water on Pt (221) and Pt (221)/$7H_2O$ could promote the formation of OCOO intermediates to enhance O_2 dissociation. On $FeO_x/Pt/TiO_2$ catalyst, Tanaka et al. (2015) believed that CO catalytic oxidation followed an ionic process. As illustrated in Fig. 9, doping FeO_x species on Pt/TiO_2 catalyst accelerated the dissociation of H_2O into H^+ ion and OH^- ion. The CO adsorbed on the Pt site and the OH^- ion to generate HCOO (a) and electrons. The electrons combine with the dissociated H^+ ion to capture oxygen atoms from O_2 dissociation to form OH (a) on Pt sites. The reaction between HCOO (a) and OH (a) eventually releases CO_2 and H_2O. It is worth noting that the reaction of OH (a) with HCOO (a) is faster than the reaction of CO (a) with O (a) at 60 °C.

$$2\left[CO + Pt^{*} \leftrightarrow CO{-}Pt\right] \quad (15)$$

$$2[H_2O + M{-}[O] \leftrightarrow HO{-}M{-}[O]{-}H] \quad (16)$$

$$2[CO{-}Pt + HO{-}M{-}[O]{-}H \rightarrow COOH{-}Pt + M{-}[O]{-}H\,] \quad (17)$$

$$2[COOH{-}Pt \rightarrow CO_2 + Pt{-}H] \quad (18)$$

$$2\left[Pt{-}H + M{-}[O]{-}H \rightarrow Pt^{*} + M{-}[\blacksquare]{-}H + H_2O \right. \quad (19)$$

$$2M{-}[\blacksquare] + O_2 \rightarrow 2M{-}[O] \quad (20)$$

Pt^* refers to the active site on Pt. $M-[O]$ refers to the lattice oxygen on the support. $M-[\blacksquare]$ refers to oxygen vacancy on the support.

Water-Inhibited Mechanism

However, there were also reported in the literatures of the inhibitory effect of water on the catalytic oxidation of CO on Pt-based catalysts. On the Pt/TiO_2 catalyst (Liu et al. 2018a, b), the presence of 5% water vapor in the reaction atmosphere inhibited the CO catalytic activity. Liu et al. (2018a, b) reported that the introduction of water molecules led to the formation of hydrogen bonds and van der Waals forces with the intermediate product of COOH* species, resulting in the COOH* species could not be easily decomposed.

Au-based catalysts

Effect of catalyst support

Catalyst support greatly affects the performance of gold-based catalysts for the catalytic oxidation of CO. Fujita et al. (2019) reported that Au/ZnO catalyst has excellent CO oxidation activity at low temperature. Ha et al. (2018) prepared nano-gold catalysts supported by different CeO_2 crystal facets. Among

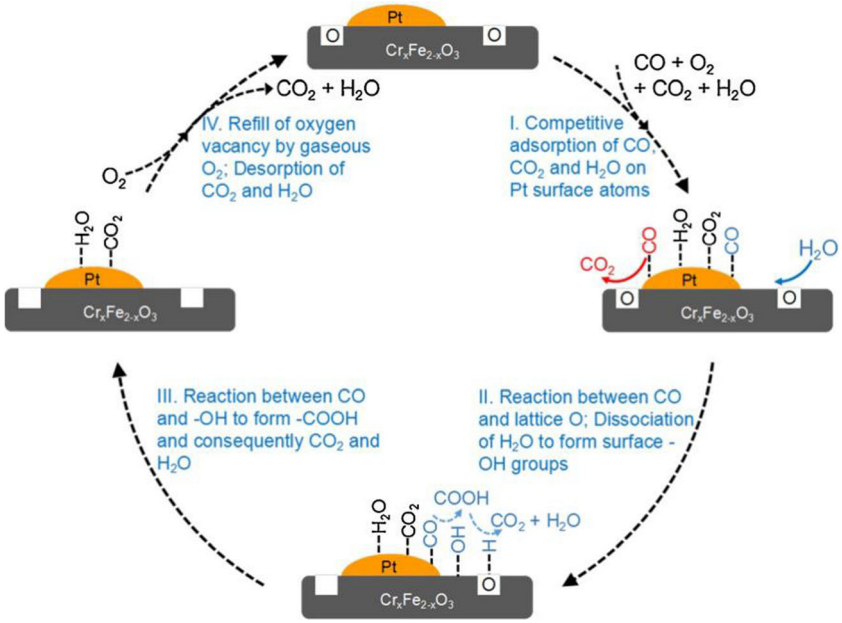

Fig. 8 Reaction pathways of CO oxidation over $Pt/Cr_{1.3}Fe_{0.7}O_3$ catalyst under different conditions (Wang et al. 2019). Copyright 2019, Elsevier

them, Au/CeO_2 (100) showed better CO catalytic oxidation activity than Au/CeO_2 (111). The Arrhenius equation revealed that the catalytic oxidation of CO on both catalysts followed the MvK mechanism, indicating that the crystal formation of the support significantly affects the catalytic activity of the catalyst. Gold catalysts loaded on the reducible supports showed excellent CO catalytic oxidation activity at low temperature, which is because the reducing support is easier to activate oxygen. Therefore, it seems that reduction with H_2 is an effective strategy to obtain higher CO oxidation activity, but this method does not seem to be suitable for the catalytic oxidation of CO in actual industrial flue gas. Besides, Liu et al. (2016) reported that gold supported on non-reducing phosphate supports (Au/La-P-O-NW) also showed great activity

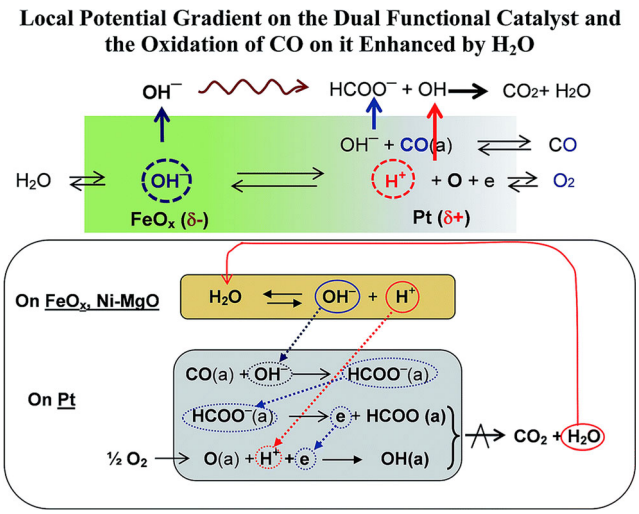

Fig. 9 Proposed reaction pathways for CO oxidation on $FeO_x/Pt/TiO_2$ catalyst at 60 °C (Tanaka et al. 2015). Copyright 2015, RoyalSociety of Chemistry

of oxidation at low temperature. Comotti et al. (2006) prepared supported gold-based catalysts loaded on four supports (TiO_2, Al_2O_3, ZrO_2, and ZnO) for CO catalytic oxidation. Among them, Au/TiO_2 and Au/Al_2O_3 showed more excellent catalysis activity. Akita and Maeda (2018) prepared the $Au/SrTiO_3$ catalyst by deposition precipitation method, and it showed excellent CO catalytic oxidation activity at room temperature.

Effect of dopant and metal alloy

Dopant also has a significant effect on the catalytic oxidation of CO for gold-based catalysts. Guo et al. (2018) reported Au/M-TiO_2 NTs (M = Ce, Ga, Co, Y) catalysts for the oxidation of CO. These four dopants all promoted the performance of CO catalytic oxidation, of which Y element doping gave the best activity of CO oxidation. Ma et al. (2007) prepared $Au/M_xO_y/TiO_2$ catalysts for CO catalytic oxidation (M_xO_y = CaO, NiO, ZnO, Ga_2O_3, Y_2O_3, ZrO_2, La_2O_3, Pr_2O_3, Nd_2O_3, Sm_2O_3, Eu_2O_3, Gd_2O_3, Dy_2O_3, Ho_2O_3, Er_2O_3, Yb_2O_3 or SiO_2-WO_3), doping CaO, NiO, ZnO, Ga_2O_3 and rare earth elements not only promote the oxidation activity of CO but also improve the anti-sintering ability of the samples. Lu et al. (2020) reported Ni-doped Au/Al_2O_3 catalyst (Au/Ni_xAl) was used for CO catalytic oxidation, in which $Au/Ni_{0.05}Al$ catalyst showed the highest CO oxidation activity, and the complete conversion temperature of CO was 20 °C. Yang et al. (2016) reported that Zr- and La-doped Au/CeO_2 catalysts were used for CO catalytic oxidation. The Zr- and La-doped $Au/CeZrLaO_x$ catalysts exhibited more excellent CO oxidation owing to that Zr and La doping enhanced the metal-support interaction, forming more oxygen vacancies, which was consistent with the XPS results. Rodriguez et al. (2018) prepared

Au/K/o-TiO_2 (110) catalyst with K doping, which not only improved the activity of CO oxidation but also created a new CO oxidation pathway, as shown in Eq. 21. In addition, metal alloy catalysts were also prepared for high CO catalytic activity. The catalytic activity of the alloy catalyst was related to the ratio of the two metals. Li et al. (2018) reported that Au-Pt/TiO_2 SNT alloy catalyst was used to CO oxidation. When the Au/Pt ratio was 5 with the calcination temperature at 400 °C, the catalytic activity was excellent with T_{100} = 80 °C. Xu et al. (2010) prepared Au-Pd alloy catalysts with different compositions for CO catalytic oxidation, of which $Pd_{90}Au_{10}$ and $Pd_{31}Au_{69}$ catalysts gave excellent CO catalytic oxidation activity at 27 °C.

$$2CO \rightarrow C_{ads} + CO_{2,ads} \quad (21)$$

Effect of physicochemical properties

The physicochemical properties of gold-based catalysts are also important factors that affect catalytic performance. Haruta et al. (1993) found that the catalytic activity of the supported gold-based catalyst for CO oxidation was apparently related to the size of the gold nanoparticles. The catalytic activity of nanoparticles less than 5 nm increased significantly. The reduction of gold nanoparticle size results in increasing the number of low-coordinate Au sites (which is beneficial for the adsorption of activation CO) and increasing in the length of the metal-support interface (which is beneficial for the activation of oxygen). As shown in Fig. 10, Yao et al. (2016) deposited different thicknesses of ultrathin TiO_2 overcoats onto three Au/TiO_2 catalysts to increase the length of metal-support interface using atomic layer deposition (ALD). XPS results showed that Au/TiO_2-S (2.9 ± 0.6 nm), Au/TiO_2-M (5.0 ± 0.8 nm), and Au/TiO_2-L (10.2 ± 1.6 nm) catalysts were mainly still in metallic state, indicating that TiO_2 atomic layer coverage did not change the charge properties of Au nanoparticles. However, in situ FTIR results showed that with the coverage of TiO_2 atomic layer, the number of CO adsorption sites was considerably reduced. The number of low-coordinated Au sites of uncoated Au/TiO_2-M and Au/TiO_2-L was two orders of magnitude higher than that of Au/TiO_2-S coated with TiO_2 layer. However, the activity comparison found that the CO conversion of Au/TiO_2-S catalyst at 25 °C was higher than Au/TiO_2-M and Au/TiO_2-L.

Therefore, it could be seen that the reason why the reduction in the size of the gold nanoparticles led to a stronger catalytic activity was that the length of the metal-support interface was increased. It was also speculated that the activation of oxygen at the metal-support interface was the rate-controlling step for CO catalytic oxidation. In addition, the

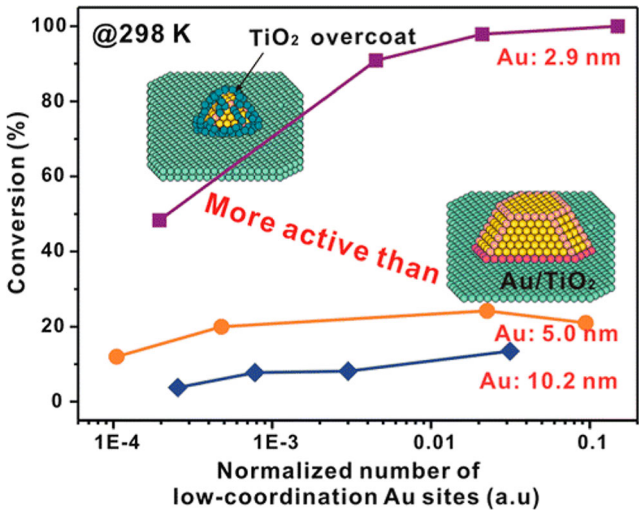

Fig. 10 CO conversion as a function of the number of exposed low-coordination Au sites on Au/TiO_2-S, Au/TiO_2-M, and Au/TiO_2-L catalysts at 25 °C (Yao et al. 2016). Copyright 2016, American Chemical Society

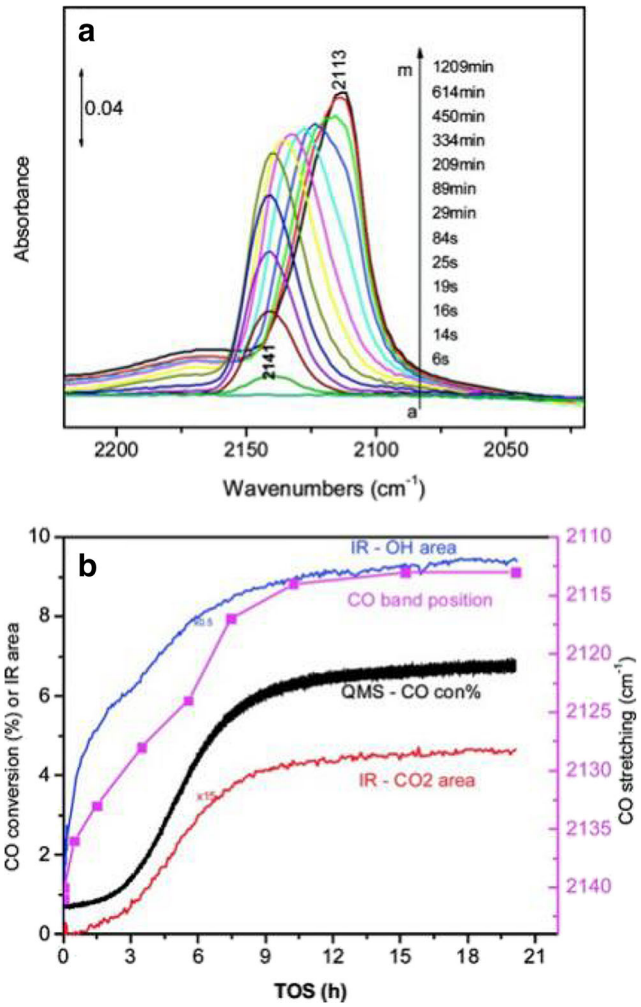

Fig. 11 (A) IR spectra during rt CO oxidation on 500 °C O_2-treated Au/SiO_2. (B) Plots of IR CO_2 area, QMS CO conversion, IR CO band position, and IR -OH band area as a function of reaction time during room temperature CO oxidation on 500 °C O_2-treated Au/SiO_2 (Wu et al. 2009). Copyright 2009, American Chemical Society

low-coordination metal Au species seem to be more capable for catalyzing CO oxidation than Au^+ species. For instance, as shown in Fig. 11, Wu et al. (2009) found that the CO adsorption bond was red-shifted from 2142 cm^{-1} ($Au^{\delta+}$-CO) to 2113 cm^{-1} (Au^0-CO) on the Au/SiO_2:O_2-treated sample, which was attributed to the gradual reduction $Au^{\delta+}$ to Au^0. Meanwhile, mass spectrometry showed that the CO adsorbed on the metallic Au showed (Au^0-CO) better reactivity, suggesting that metal Au^0 species played an important role in the catalytic oxidation of CO at room temperature. Wei et al. (2018) found that the CO conversion on the Au^{n+}/TiO_2 ($1 < n < 3$) catalyst increased with time extension. The results of in situ diffuse-reflectance infrared Fourier transform spectroscopy (in situ DRIFTS) showed that Au^{n+} species gradually reduced to Au^0 species in the catalytic oxidation process of CO. In addition, the results of in situ Raman spectroscopy indicated that during the reduction of Au^{n+} species to Au^0 species, more oxygen vacancies were formed on the TiO_2 support, which was conducive to O_2 activation. As we all know, the single-atom Au exists as the $Au^{\delta+}$ species. However, many literatures reported that the single-atom Au catalyst also exhibited excellent CO catalytic performance. Based on the first-principles calculations, Shi et al. (2017) found that single-atom gold supported on oxygen vacancies of TiO_2 support gave excellent CO catalytic oxidation performance, which was attributed to the unique electronic effect of Au atoms. In addition, Zhao et al. (2019) reported that under the promotion of water vapor, the single-atom Au/CeO_2 catalyst showed better CO catalytic oxidation ability than Au NP catalysts due to the unique local atomic structure and electronic properties of gold atoms. The single-atom Au located at the Ce vacancy sites could bond with three coordinated unsaturated oxygen atoms to form a highly positively charged state, while the Au atom located at the metal-support interface on Au NP catalysts could only bond with one O atom. The positively charged Au_1 atom has a flexible valency change ability ($Au^{3+} \rightarrow Au^{2+} \rightarrow Au^+$) which was beneficial to the reaction between CO and -OH groups.

Effect of harsh reaction conditions

The reaction atmosphere also has an important influence on the performance of Au-based catalysts for CO catalysis. Rutha et al. (2000) found that SO_2 greatly inhibited the catalytic activity of CO on Au/TiO_2 catalyst under low-temperature conditions (<0 °C). After treatment at 0 °C for 3 h for Au/TiO_2 catalyst, the apparent activation energy of CO oxidation increased significantly. Generally, Pt/TiO_2 catalyst contributed poorer low-temperature activity than Au/TiO_2. It was found that sulfation treatment of Pt/TiO_2 catalyst led to slight increase of complete oxidation temperature of CO from 100 to 130 °C. However, for Au/TiO_2 catalyst, its catalytic activity apparently decreased, showing dramatic increase of complete oxidation temperature of CO from 0 to 150 °C. In order to explore inhibition mechanism of SO_2 on CO catalytic oxidation, XPS characterization found that the metal interface seriously accumulated sulfate species on the used Au/TiO_2 samples (Kim and Woo 2006). Through in situ FTIR experiments, it was found that the sulfate species accumulated at the Au-TiO_2 interface occupied the active sites, thereby inhibiting the formation of intermediate carbonate species. It is worth noting that the XPS characterization revealed that the valence state of Au species did not change before and after use, indicating that active Au species are not easy to be sulfated. Clark et al. (2013) prepared Au and La_2O_3 catalysts supported on TiO_2 nanofibers in different orders, and investigated their CO catalytic activities in a typical Claus tail gas atmosphere (1.6% CO, 1.5% H_2, 13.2% CO_2, 22.0% H_2O, 4.1% O_2, 1% H_2S, 0.2% SO_2, 0.05% COS, 0.02% CS_2) at 300–400 °C. The catalysts with Au supported on La_2O_3/TiO_2 support (Au/La_2O_3/TiO_2-NFs-1) gave better CO catalytic activity than Au and La_2O_3 deposited on TiO_2 support (Au/La_2O_3/TiO_2-NFs-2). The results of FTIR spectra confirmed that sulfate species were only deposited on the used Au/La_2O_3/TiO_2-NFs-2 catalyst. Under the reaction conditions of Claus tail gas (0.64% H_2S, 0.29% SO_2, and 16.74% H_2O) at 300–350 °C, the 1%Au/Eu_2O_3/TiO_2 catalyst (Kazemi et al. 2019) has a significantly better CO oxidation activity than the 1%Au/TiO_2 catalyst. The results of ion chromatography (IC) measurement showed that the sulfate species on the Au/Eu_2O_3/TiO_2 catalyst were lower than the Au/TiO_2 catalyst, indicating that the Eu_2O_3-doped Au/TiO_2 catalyst was beneficial to inhibit the deposition of sulfate on the catalyst. This is due to the doping of the lanthanide oxides which makes the Au/TiO_2 catalyst form more oxygen vacancies and inhibits the adsorption of SO_2. However, it is worth noting that Au/Eu_2O_3/TiO_2, Au/Er_2O_3/TiO_2, Au/TiO_2, and Au/La_2O_3/TiO_2 catalysts all showed very low CO catalytic oxidation activity at 200–250 °C. The in situ FTIR results demonstrated that the low reaction temperature leads to more serious sulfate accumulation on the catalyst. Therefore, catalytic oxidation of CO under high-temperature conditions (300–350 °C) is more conducive to reducing the deposition of sulfate species on the catalyst. Valechha et al. (2017) reported the influence of the presence of 10 ppm SO_2 in the reaction atmosphere on the CO catalytic oxidation activity of Au/CeO_2 catalysts at 40 °C. The Au/$Ce_{0.8}Zr_{0.2}O_2$ catalyst doped with Zr had a CO conversion of 55% after 18 h of sulfur aging, while the CO conversion was only 18% for sulfur-aged Au/CeO_2. After heat treatment at 150 °C for 2 h, the CO conversion of Au/$Ce_{0.8}Zr_{0.2}O_2$ catalyst was recovered to 85% while that of Au/CeO_2 was only 49.7%. Therefore, Zr-doped Au/CeO_2 catalyst could improve the sulfur resistance of the catalyst. Indeed, Au-based catalysts can effectively reduce sulfate poisoning at higher reaction temperatures, leading to high CO oxidation activity. However, the sulfate species accumulated at the metal-support interface is the principle reason for low CO activity at low temperature.

Obviously, for Au-based catalysts, there is still a lack of CO catalytic oxidation research under typical industrial flue gas conditions (100–250 °C), which greatly limits the application of Au-based catalysts to CO purification of industrial flue gas.

The effect of chloride residual on performance of CO oxidation for Au nanoparticle catalysts was investigated. Au/CeO_2 catalysts were prepared by a traditional impregnation method (IMP) and by liquid-phase reductive deposition (LPRD). It was found that Au/CeO_2 (IMP) contained 1.1% residual chlorine, which not only reduced the reduction of surface oxygen groups but also possibly facilitated the sintering of gold nanoparticles, resulting in lower CO catalytic activity (Carabineiro et al. 2010).

Reaction mechanisms

In recent years, many factors such as support, doping, Au valence, and Au nanoparticle size affecting the catalytic activity of the Au-based catalyst have been extensively researched. However, there are still many controversies regarding the activation of O_2 molecules and the role of lattice oxygen, which is very important for the catalytic oxidation of CO. As illustrated in Fig. 12, Widmann and Behm (2013) summarized three reaction mechanisms (Au-only mechanism, interface mechanism, and MvK mechanism) for CO catalytic oxidation on Au/Oxides catalyst in the reaction atmosphere without water. As shown in Fig. 12 A, CO is adsorbed on the Au sites, and the active oxygen species are derived from oxygen molecules or oxygen atoms adsorbed on the Au NPs. As illustrated in Fig. 12 B and C, the reactive oxygen species adsorbed at the metal interface or oxygen vacancy react with CO to form CO_2. Obviously, the reaction molecules are all adsorbed, which conforms to the typical L-H Mechanism. As illustrated in Fig. 12 D, the lattice oxygen on the support as active oxygen species reacts with CO to generate CO_2. Therefore, this pathway conforms to the typical MvK mechanism.

Langmuir-Hinshelwood mechanism

When Au is loaded on the metal oxides, under normal conditions, CO is adsorbed and activated at the low-coordinate Au sites ($T > 25$ °C). However, when the temperature is very low, CO is more easily chemisorbed on the support other than the low coordination Au sites. O_2 is either dissociated into two oxygen atom or molecular chemisorption to become active oxygen species. CO is also chemically adsorbed on the low-coordinated Au sites. At present, it is generally believed that on Au/Oxides catalyst, O_2 adsorption is more stable at low temperature (T<0 °C) and lattice oxygen is not easy to form oxygen vacancies to participate in CO catalytic oxidation. Therefore, under low-temperature conditions (T<0 °C), CO catalytic oxidation on Au/oxide catalysts follows the L-H mechanism. Gogate (2019) believed that the dissociation

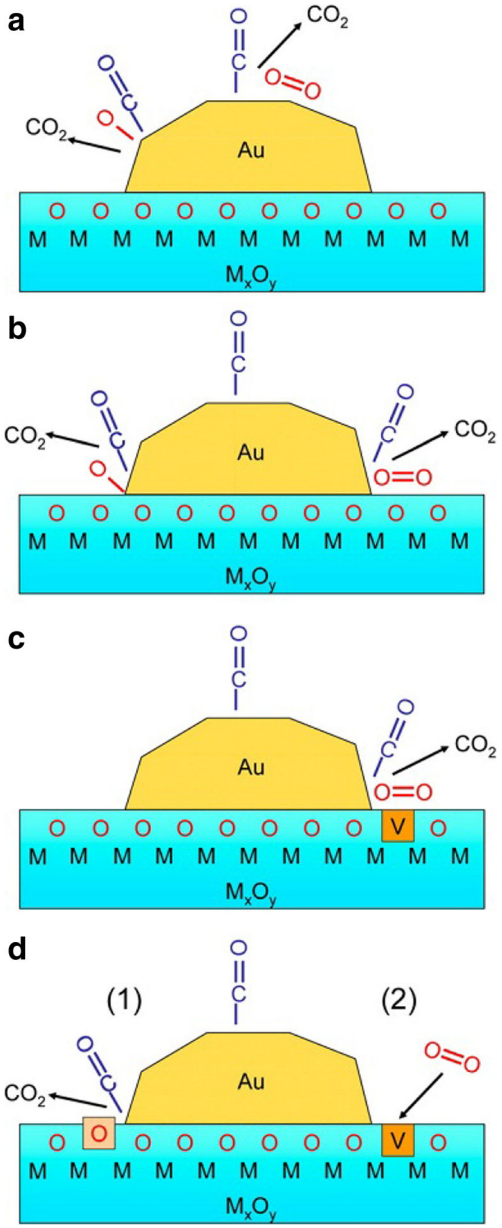

Fig. 12 Possible reaction path of CO on supported Au catalyst (Widmann and Behm 2013). Copyright 2013, American Chemical Society

energy (250 kJ/O_{atom}) of O_2 adsorbed on Au sites was very high. Therefore, it was considered that the direct dissociation of O_2 as a pathway for the reaction between oxygen atoms and CO was thermodynamically infeasible. As shown in Fig. 13, Green et al. (2011) proposed the reaction mechanism of CO oxidation on Au/TiO_2 catalyst at low temperature through DFT calculations and experiments. O_2 chemisorption on the metal-support interface to form Au-O-O-Ti species was activated. When the temperature was lower than − 153 °C, CO chemically adsorbed on the support TiO_2 (CO/TiO_2) was more likely to react with O_2 activated on the metal-support interface. When the temperature was higher than − 153 °C, CO chemically adsorbed on the Au sites (CO/Au) participated

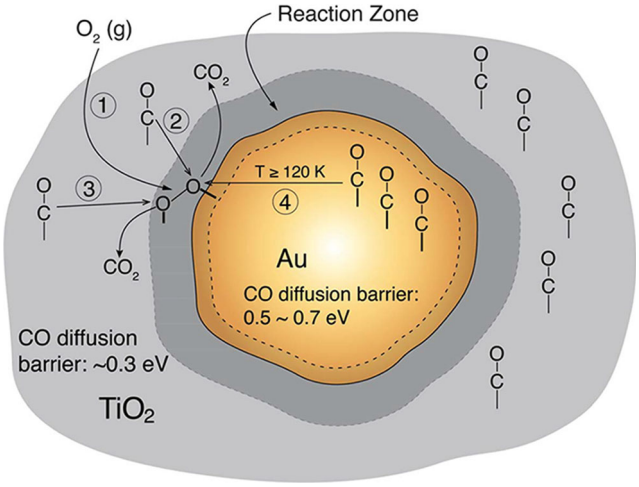

Fig. 13 Schematic diagram of the mechanism of low-temperature CO oxidation on the reactive surrounding area on Au/TiO_2 catalyst (Green et al. 2011). Copyright 2011, Science

in the reaction. The intermediate product of the reaction was considered to be $O{=}C{\cdots}O_2$ species. Besides, it has been reported that O_2 was activated at the metal interface or oxygen vacancies to participate in the CO oxidation reaction. Carrettin et al. (2007) reported that the Fe-doped Au/TiO_2 catalyst formed more oxygen vacancies near iron to enhance the performance of CO oxidation. Raman spectroscopy detected that the formation of superoxide radicals and peroxygen radicals on the oxygen vacancies by O_2 is the fundamental reason for the enhancement of catalytic activity. When the temperature is lower than − 25 °C, after the H_2 reduction on the Au/ZnO catalyst and then the O_2 pretreatment, UV-vis spectroscopy suggested that more oxygen vacancies were formed on the catalyst and electron paramagnetic resonance (EPR) results demonstrated that weakly adsorbed O_2 species (O_2^- radicals) were formed on the oxygen vacancies resulting in enhancing catalyst activity (Fujita et al. 2019). Additionally, as shown in pathway 2 of Fig. 14, Schubert et al. (2001) proposed on Au/Fe_3O_4 catalyst: (1) Oxygen molecules adsorbed on the support and migrated to the metal interface to dissociate into adsorbed oxygen atoms or form O_2^- species; (2) adsorbed oxygen atoms or peroxide species (O_2^-) react with CO adsorbed on the Au sites to product CO_2.

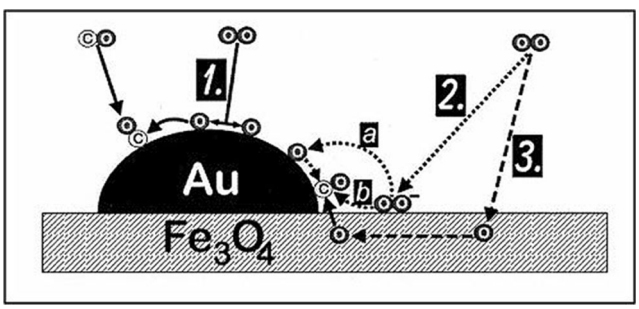

Fig. 14 Possible reaction path for CO oxidation on Au/Fe_3O_4 catalyst (Schubert et al. 2001). Copyright 2001, Elsevier

Mars-van Krevelen mechanism

When the temperature is higher than 25 °C, many literatures commonly indicated that the lattice oxygen on the support participates in the catalytic oxidation reaction of CO as the active species when the Au nanoparticles are supported on the reducible support (carriers with low oxygen vacancy formation energy or strong oxygen storage capacity). The catalytically active sites of CO catalytic oxidation through the MvK reaction pathway are still controversial. Bond and Thompson carefully considered that weakly bonded lattice O_2^- ions on oxygen vacancies were oxidants for CO oxidation over Au catalysts supported on reducible carriers (Bond and Thompson 2001, 2009). The -OH groups on the carrier attacked the adsorbed CO to form Au-COOH species and oxygen vacancies. O_2 weakly bonded with carrier cations to form lattice O_2^- ions. The interaction between Au-COOH species and lattice O_2^- ions generated CO_2. As a consequence, the reaction steps are illustrated in Eqs. 22–28:

$$2\left(Au^0 + CO \rightarrow Au^0{-}CO\right) \tag{22}$$

$$2\left(Au^{3+} + OH_s^- \rightarrow Au^{3+}{-}OH\right) \tag{23}$$

$$2\left(Au^0{-}CO + Au^{2+}{-}OH \rightarrow Au^{2+}{-}COOH + Au^0\right) \tag{24}$$

$$O_2 + \square_s^- \rightarrow O_2^-{-}\square_s \tag{25}$$

$$Au^{2+}{-}COOH + O_2^-{-}\square_s \rightarrow Au^{2+} + CO_2 + HO_2^-{-}\square_s \tag{26}$$

$$Au^{2+}{-}COOH + HO_2^-{-}\square_s \rightarrow Au^{2+} + CO_2 + 2OH_s^- + \square_s \tag{27}$$

$$Au^{2+} + \square_s \rightarrow Au^{3+} + \square_s^- \tag{28}$$

□ refers to oxygen vacancy.

Duan and Henkelman (2018) proposed three possible MvK reaction pathways for CO on Au/TiO_2 catalyst by DFT calculations and believed that the O-Au-CO species formed at the metal interface was the active site of the reaction and the dissociation of the O_2 molecule (supplement of lattice oxygen) was the rate-controlling step. Carbonate species formation at the O_{top}/Ti_{5c} sites was the main reason for catalyst deactivation. Based on the measurement results of quantitative temporal analysis (TAP) of product reactor, Widmann and Behm (2013) believed that when the reaction temperature was higher than 80 °C, lattice oxygen at the metal interface of the Au/TiO_2 catalyst was provided as active oxygen species. Besides, the CO oxidation by MvK reaction pathway of O_{latt}-C-O species as an intermediate product was proposed on Au/CeO_2 and Au/TiO_2 (Ha et al. 2018; Schlexer et al. 2018).

Water-Assisted Mechanism

For Au-based catalysts, numerous reports showed that H_2O promoted the catalytic oxidation of CO. The Water-Assisted Mechanism was classified into three types: (1) The dissociation of water on the gold-based catalyst into the -OH groups is adsorbed on the Au site or on the support site near Au via the pathway (COOH* + OH* → CO_2 + H_2O) participated in the CO catalytic oxidation reaction. Kim et al. (2006) through isotope-labeling experiments found at a low temperature of − 196 °C, the Au (111) surface was covered with 0.18 ML ^{16}O and 0.1 ML $H_2{}^{18}O$ in advance, and then 0.18 ML CO was injected. The results of mass spectrometry found that $C^{16}O^{18}O$ with a mass of 46 accounted for 27% of the total CO_2. It proved that when oxygen atoms were pre-adsorbed on the Au (111) surface, H_2O directly participated in the catalytic oxidation of CO. And the author believed that -OH groups formed by the interaction of atomic oxygen with H_2O participate in the formation of CO_2. On the Au/CeO_2 single-atom catalyst, Zhao et al. (2019) found by operando diffuse-reflectance Fourier transform infrared (DRIFT) and DFT calculations that the -OH groups (3667 cm^{-1}) on the CeO_2 carrier are gradually consumed in absence of water vapor in reaction atmosphere. At this time, the pathway of CO + OH → COOH→CO_2 + H gave the lowest energy barrier needed to overcome for the catalytic oxidation of CO. However, when the -OH groups on the carrier were gradually consumed, the lattice oxygen acted as an active oxygen species for the catalytic oxidation of CO. Meanwhile, the reaction pathway of the catalytic oxidation of CO was CO + O_L → CO_2 + O_V. When 2% water vapor was introduced into the gas flow, the water vapor was dissociated into -OH groups at CeO_2 surface, and the CO adsorption peak gradually disappears. Therefore, the -OH groups generated by the hydrolysis was used as the active oxygen species for the catalytic oxidation reaction of CO. Furthermore, as shown in Fig. 15, according to the DFT calculations, the corresponding reaction mechanism of water vapor promoting the catalytic oxidation of CO was proposed over the Au/CeO_2 SAC. Meanwhile, the reaction pathway of CO catalytic oxidation was COOH* + OH* → CO_2 + H_2O. (2) Dissociation to -OH functional groups and protons on catalyst promoted O_2 activation. A study (Liu et al. 2006) has shown that water could be easily dissociated into -OH groups on the oxygen vacancies of the support TiO_2. The dissociated -OH groups provided electrons to the support to accelerate the adsorption of O_2 on the support TiO_2, and O_2 as active oxygen species migrated along the support participate in CO catalytic oxidation reaction. As shown in Fig. 16, another view was that the hydrolysis ion provides protons to the O_2 adsorbed at the metal-support interface to form the intermediate product OOH species, which greatly reduces the energy required for O–O bond breakage (Saavedra et al. 2018). (3) Accelerating the decomposition of intermediate products. There was also a view that water promoted the conversion of intermediate carbonate species to bicarbonate species, which was easily decomposed, thereby improving the catalytic activity of Au-based catalysts in a wet reaction atmosphere (Date et al. 2004; Nakamura and Fujitani 2014). As clarified in Fig. 17, the reaction path is (1) O_2 adsorbed on the support migrates to the metal-support interface and is activated to form active oxygen species; (2) CO adsorbed on the Au sites reacts with the activated oxygen to generate carbonate species (CO_3); (3) carbonate species and the protons generated by hydrolysis form easily decomposed bicarbonate species (CO_3H).

Pd-based catalysts

Effect of catalyst support

In recent years, Pd-based catalysts have attracted extensive attention especially in the purification of diesel exhaust. Their catalytic performance for CO oxidation is greatly affected by the support. Khder et al. (2019) prepared Pd/Mn_3O_4 catalysts with different loading of Pd (2% or 4%) for CO catalytic oxidation. Among them, the 4%Pd/Mn_3O_4 catalyst without hydrothermal treatment of the support gave the highest catalytic activity (T_{100} = 20 °C), and exhibited great stability. Mao et al. (2019) prepared NiO, Co_3O_4, Fe_2O_3, MnO_2, CeO_2, and ZrO_2 monolayers on γ-Al_2O_3 as a support by Atomic Layer Deposition (ALD) method to prepare 1% Pd/M_xO_y/γ-Al_2O_3 for CO catalytic oxidation. Among them, Pd/CeO_2/γ-Al_2O_3, Pd/Fe_2O_3/γ-Al_2O_3, and Pd/MnO_2/γ-Al_2O_3 could promote the catalytic oxidation of CO compared with Pd/γ-Al_2O_3 catalysts. Zhai et al. (2018) used three different forms of TiO_2 support (TiO_2 microspheres with a diameter of about 2.2 μm, P25, and commercial anatase) to load about 1% Pd/TiO_2 catalyst for CO catalytic oxidation. The high specific surface area, high Pd dispersion, and strong CO adsorption and O_2 adsorption on the catalyst were the fundamental reasons for the better activity of the TiO_2 special nanosheet assembly structure catalyst. The complete conversion temperatures of CO on these three catalysts (Pd/TiO_2-350, Pd/TiO_2-P25, and Pd/TiO_2-CA) were 80, 140, and 160 °C, respectively. Wang et al. (2017a, b) supported Pd on two different types of Fe_2O_3 (α-Fe_2O_3, γ-Fe_2O_3) for CO oxidation at low temperature, of which Pd/γ-Fe_2O_3 performed better in CO catalytic oxidation (T_{100} = 0 °C). Li et al. (2020) loaded Pd on CeO_2, $Ce_{0.7}Zr_{0.3}O_2$, and$Ce_{0.3}Zr_{0.7}O_2$ supports by impregnation method for CO catalytic oxidation, of which Pd/$Ce_{0.3}Zr_{0.7}O_2$ showed the highest catalytic performance (T_{50} = 134 °C). Du et al. (2019) obtained Pd/CoO_x–InO_x catalysts for CO catalytic oxidation by impregnating Pd on nanofiber CoO_x–InO_x supports with different morphologies. Compared with Pd/CoO_x–InO_x-600 and Pd/CoO_x–InO_x-700 catalysts, Pd/CoO_x–InO_x-500 catalysts have a high specific surface area, high dispersion of Pd particles, and smaller Pd particles. Therefore, the Pd/CoO_x–InO_x-500 catalyst gave the highest

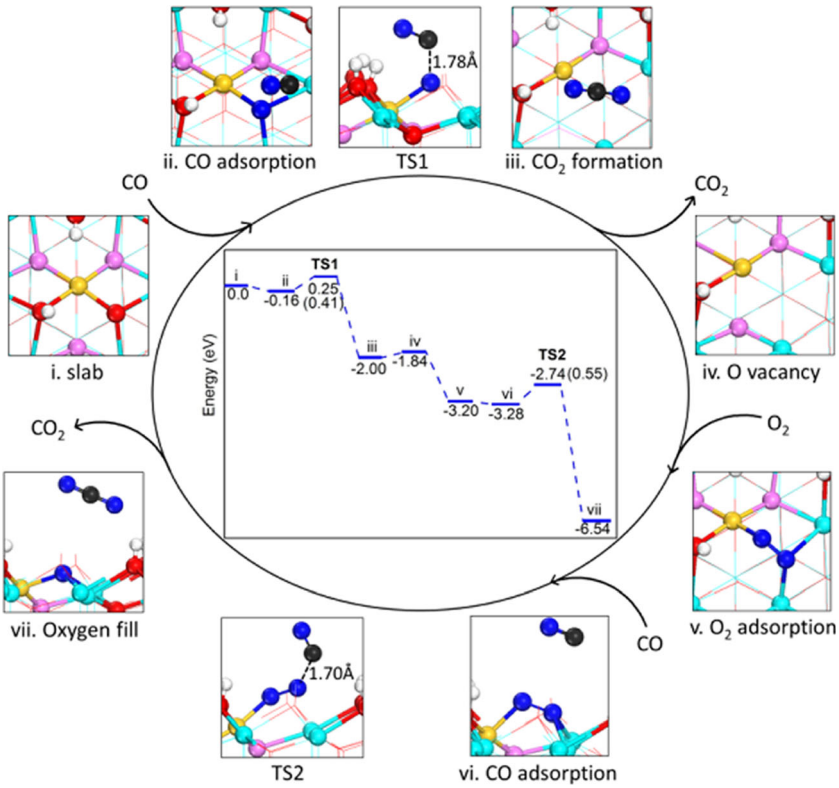

Fig. 15 The catalytic oxidation mechanism of CO in the presence of water vapor on monoatomic Au/CeO_2 catalyst (Zhao et al. 2019). Copyright 2019, Nature

CO catalytic activity (T_{50} = 52 °C). Spezzati et al. (2019) supported Pd on two different morphologies of CeO_2 (CeO_2-rods and CeO_2-cubes) by impregnation for CO catalytic oxidation. The CO complete conversion temperature on the Pd/CeO_2-rods was around 150 °C, while on the Pd/CeO_2-cubes was 200 °C.

Effect of physicochemical properties

As we all know, the CO catalytic oxidation activity of Pd-based catalysts is affected by the valence state of Pd. As shown in Fig. 18, on the 5 wt% PdO_x/γ-Al_2O_3 (x = 0–1) catalyst (Zorn et al. 2011), the Pd-Al_2O_3 and $PdO_{x<1}$-Al_2O_3 catalysts gave better CO

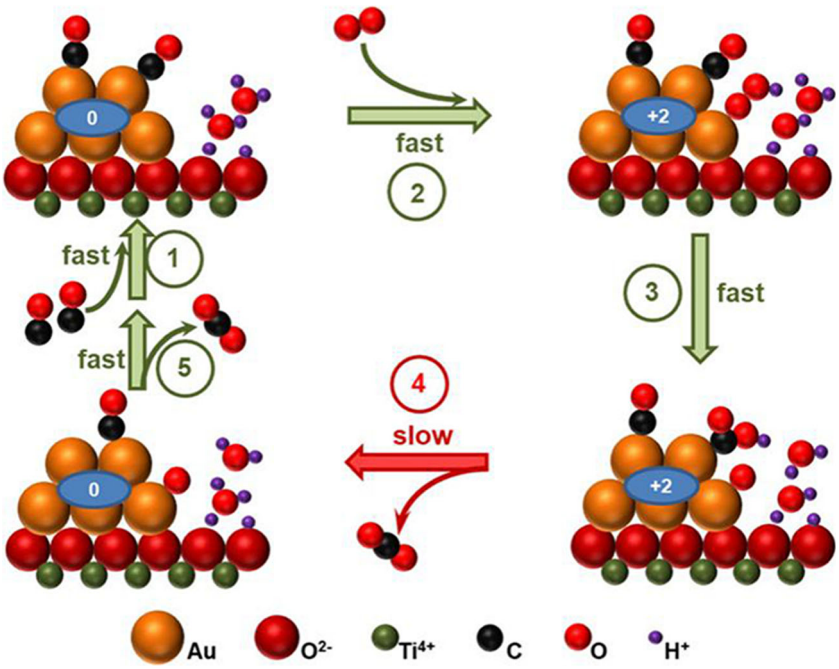

Fig. 16 Proposed mechanism of CO oxidation over supported gold nanoparticles with the water co-catalyst adsorbed on the support at the metal-support interface (Saavedra et al. 2018). Copyright 2018, American Chemical Society

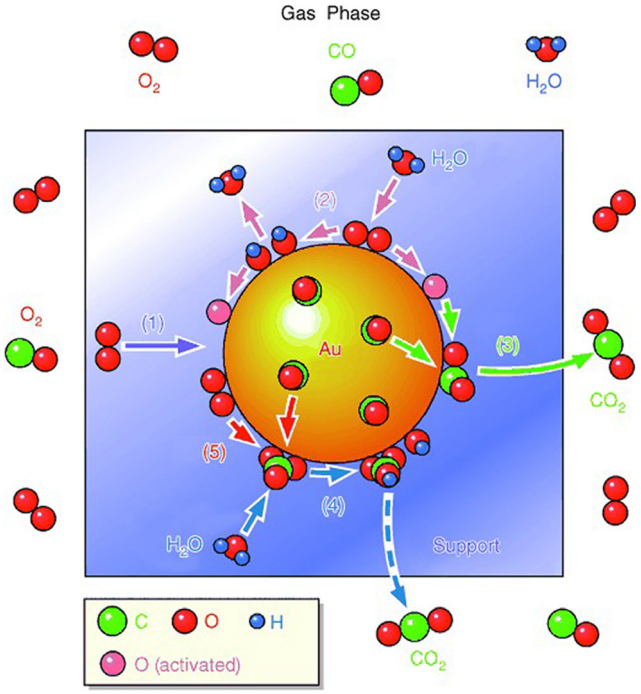

Fig. 17 Mechanism of water promoting decomposition of intermediate products (Date et al. 2004). Copyright 2004, Wiley

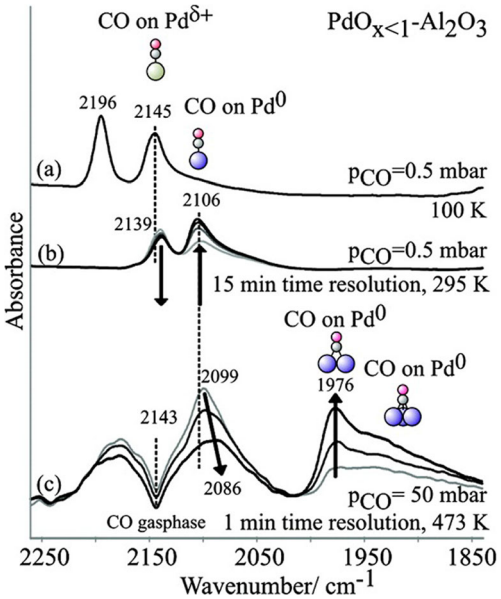

Fig. 19 In situ FTIR spectra under different reaction atmosphere conditions (Zorn et al. 2011). Copyright 2011, American Chemical Society

oxidation performance than PdO-Al_2O_3. According to the results of in situ FTIR and XRD tests, the metal Pd on the PdO/γ-Al_2O_3 catalyst was located inside the PdO nanoparticles. In addition, the pressure of CO and O_2 in the reaction atmosphere also affected the state of Pd on the catalyst. As shown in Fig. 19, according to the results of in situ FTIR experiments, PdO_x was slowly reduced to Pd^0 when under low CO pressure at 22 °C. PdO_x was quickly reduced to Pd^0 when under high CO pressure conditions at 22 °C. However, the PdO was difficult to be reduced to metallic Pd, resulting in the low CO oxidation performance of the PdO-Al_2O_3 catalyst. Therefore, weakening the metal-support interaction to obtain more metal Pd seems to be a strategy to achieve high CO catalytic performance. In addition, the particle size of Pd nanoparticles is also one of the important factors affecting CO

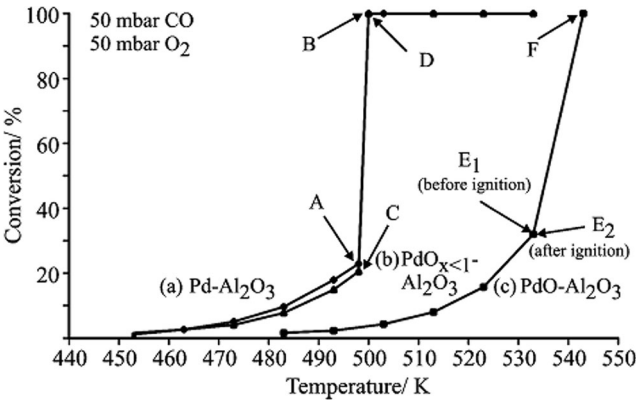

Fig. 18 CO oxidation at different temperatures. (a) Pd-Al_2O_3. (b) $PdO_{x<1}$-Al_2O_3. (c) PdO-Al_2O_3 (Zorn et al. 2011). Copyright 2011, American Chemical Society

oxidation performance. Huang et al. (2019) prepared Pd/Co_3O_4 catalysts (2.5 to 10.6 nm) with different Pd particle sizes by impregnation method (roasting at different temperatures) for CO oxidation. Among them, Pd/Co_3O_4-200 had the smallest Pd nanoparticles, thereby exhibiting the best CO oxidation activity. Based on XPS characterization, Pd/Co_3O_4-200 gave the highest Pd/PdO value (12.1%) compared to the other four samples. DFT calculations indicated that small particle sizes of Pd were beneficial to dissociate O_2 as well as desorption of product CO_2. The strong adsorption of CO by large-sized Pd particles was not conducive to the catalytic reaction. In short, obtaining a higher ratio of Pd^0/Pd^{2+} by adjusting the metal-support interaction and the calcination conditions of the catalyst is an effective method to obtain high CO catalytic activity.

Effect of harsh reaction conditions

The reaction atmosphere also has an important influence on the catalytic performance of the catalyst. Shin et al. (2018) prepared two different Ce-Zr-Al-O mixed oxides supported Pd catalysts by a single-step epoxide-driven sol-gel method (SGCZA) and co-precipitation method (PCZA). After aging at 300 °C for 3 h in an atmosphere containing 250 ppm of SO_2, TPR, FTIR, XPS results showed that the supports of these two catalysts were sulfated. In addition, the irreversible sulfation of active component and the decrease of Pd dispersion after sulfur aging are the reasons for the decrease of CO catalytic activity. After sulfur aging, the Pd/SGCZA catalyst (T_{50} = 123 °C) still showed better CO catalytic oxidation performance than Pd/PCZA catalyst. Moreover, it was also found that SO_2 caused PdO sites to form $PdSO_4$ species on Pd/Al_2O_3 catalysts, thereby considerably inhibiting the activity of CO oxidation (Mowery and

McCormick 2001). Ryou et al. (2015) investigated the application of Pd/(Ce-Zr)O_2 catalysts with different Ce/Zr ratios for the catalytic oxidation of CO. Through sulfur aging and regeneration process, it was found that the formation of Ce-Zr solid solution by Zr doping was beneficial to the stability of the catalyst. But it reduced the oxygen storage capacity of the catalyst. More importantly, after sulfur aging, a large amount of $Ce(SO_4)_2$ was formed on the Pd/CeO_2. After heat treatment, there was still residual sulfur on the surface of the catalyst, causing the CO catalytic activity not full recovery. In contrast, the Pd/$Ce_{0.58}Zr_{0.42}O_2$ catalyst showed better CO catalytic performance after sulfur aging and regeneration. Wang et al. (2015) prepared Pd/CeO_2, Pd–MnO_x–CeO_2 (Pd–MC), Pd–SnO_2–MnO_x–CeO_2 (Pd–SMC) catalysts by impregnation method for CO catalytic oxidation. The Pd-MC and Pd-SMC catalysts exhibited CO conversion over 90% at room temperature. In addition, the effects of SO_2 and water vapor on the activity of the Pd-MC and Pd-SMC catalysts were investigated. Compared with dry reaction conditions, the catalytic activity of CO did not change on Pd-SMC catalyst when 8% water vapor was introduced into the reaction atmosphere. However, in presence of 200 ppm SO_2 in reaction atmosphere at room temperature, the Pd-MC catalyst loses its activity after 100 min, and the Pd-SMC catalyst loses its activity after 130 min. Jeong et al. (2017) used hydrothermal treatment of Pd/CeO_2 catalyst to generate more -OH groups on the support to suppress the poisoning caused by sulfated surface of the support and the active site covered by carbonate species. More importantly, the Pd/CeO_2 catalyst that has undergone hydrothermal treatment at 750 °C for 25 h gave CO conversion over 80% in the stability test with 100 ppm SO_2 and maintained for 60 h. However, the Pd/CeO_2 catalyst that has not undergone hydrothermal treatment completely loses its activity after 35 h. In situ FTIR results revealed that the sulfate species on the 2% Pd/CeO_2 treated with hydrothermal treatment were significantly lower than on the as-made Pd/CeO_2. Gaudet et al. (2013) reported that La-doped Pd/γ-Al_2O_3 catalyst was used for CO catalytic oxidation, in which Pd/La-γ-Al_2O_3 catalyst had higher dispersion of Pd nanoparticles, showing higher CO catalytic activity. Doping La also suppressed the poisoning caused by excessive adsorption of CO. Hence, the main challenges are that Pd can be easily sulfated into $PdSO_4$ species and the reducible carriers are sulfated to lose the oxygen storage capacity.

Reaction mechanisms

Many literatures reported several reaction mechanisms of CO on supported Pd-based catalysts. On the Pd/Fe_3O_4, Pd/Fe_2O_3, and Pd/Co_3O_4 catalysts (Huang et al. 2019; Jain and Madras 2017), CO catalytic oxidation followed the L-H mechanism. CO adsorption on Pd sites was activated and reacted with dissociated O atoms. The specific steps were as follows: (1) CO adsorption and activation on Pd sites; (2) O_2 adsorption and dissociation into oxygen atoms (O_{ads}) on Pd sites; (3) reaction between CO_{ads} and O_{ads} to form CO_2; (4) CO_2 desorption. On the Pd/CeO_2 catalyst (Spezzati et al. 2019), the active oxygen species of CO catalytic oxidation under high-temperature conditions was lattice oxygen; therefore, the reaction pathway of CO oxidation followed the MvK mechanism. Pd atoms were inserted into the lattice to form Pd–O–Ti bonds by the solution combustion method to prepare $Ti_{1-x}Pd_xO_{2-x}$ (x = 0.01−0.03) catalyst (Mukri et al. 2012). The active oxygen species were the lattice oxygen of the $Ti_{1-x}Pd_xO_{2-x}$ (x = 0.01−0.03). The reaction pathway of CO catalytic oxidation is shown in Eqs. 29–30.

$$Ti_{1-x}Pd_xO_{2-x} + \delta CO \rightarrow Ti_{1-x}Pd_xO_{2-x-\delta} + \delta CO_2 \quad (29)$$

$$Ti_{1-x}Pd_xO_{2-x-\delta} + {}^{\delta}/_{2}O_2 \rightarrow Ti_{1-x}Pd_xO_{2-x} \quad (30)$$

Ag-based catalysts

Effect of catalyst support

The support plays an important role in the performance of CO oxidation for the Ag-based catalyst. Kolobova et al. (2017) investigated the effect of zeolite-supported Ag catalysts with different chemical compositions (Si/Al ratio = 30, 50, and 80) on the catalytic performance of CO at low temperature. Among them, Ag/ZSM-5 (Si/Al = 80) showed the highest CO catalytic activity (T_{90} = 40 °C). The number of Bronsted acid sites was decreased with increasing Si/Al ratio, resulting in increasing of CO oxidation activity. Afanasev et al. (2012) studied the performance of low-temperature CO catalytic oxidation of Ag nanoparticles supported on fumed silica catalysts, and the complete CO conversion temperature was 30 °C. Dutov et al. (2016) prepared Ag/SiO_2 catalysts by impregnation method and calcined them at different temperatures (500 or 900 °C). Among them, Ag/SiO_2-900 showed more excellent CO catalytic oxidation performance than Ag/SiO_2-500 catalyst. The results of H_2-TPR and O_2-TPO indicated that there were more active oxygen species on the Ag/SiO_2-900. Xu et al. (2017) supported Ag nanoparticles on different forms of mesoporous SiO_2 (KCC-1, SBA-15, and MCM-41). The Ag nanoparticles were anchored on mesoporous, thereby inhibiting its migration and sintering to form smaller nanoparticles, leading to the best CO catalytic performance. Grabchenko et al. (2020) prepared Ag/CeO_2 catalysts by three different methods (impregnation, impregnation of pre reduced, and co-deposition precipitation). The strength of the metal-support interaction was the key factor for the performance of CO oxidation for these three samples. Among them, the Ag/CeO_2 (red-imp) catalyst showed the best CO catalytic oxidation performance, owing to the strongest metal-support interaction resulting in forming more oxygen vacancies on the support. Qu et al. (2013) prepared CeO_2 support by hard template method and surfactant template method and supported Ag nanoparticle for CO catalytic oxidation. The complete CO conversion

temperature on Ag/CeO_2-HP was 65 °C, while Ag/CeO_2-SP was 150 °C. This was because more oxygen vacancies and O_2^- species were formed on the Ag/CeO_2-HP, which is beneficial for stabilizing and dispersing Ag nanoparticles. In addition, according to the EPR characterization, a pathway for the gas-phase O_2 molecule to supplement the lattice oxygen was proposed, as illustrated in Eq. 31:

$$O_2(gas) \leftrightarrow O_2(ad) \leftrightarrow O_2^-(ad) \leftrightarrow O_2^{2-}(ad) \leftrightarrow 2O^-(ad) \leftrightarrow 2O^{2-}(lattice) \quad (31)$$

Konopatsky et al. (2018) loaded Ag nanoparticles on different forms of boron nitride (BN). The Ag/BN 1 catalyst showed highest CO catalytic activity (T_{100} = 194 °C). Lee et al. (2018a, b) prepared three different Ce/Zr ratio nanofiber carrier supported Ag nanoparticle by typical electrospinning method for CO catalytic oxidation. Among them, the $Ag/Ce_{0.67}Zr_{0.33}O_2$ catalyst with the highest Ce/Zr ratio gave the best performance of CO oxidation (T_{50} = 282 °C), because the high Ce/Zr ratio enhanced the redox ability of the catalyst. Khan et al. (2015) prepared Ag-Sn/CeO_2 (Sn = 1–4 wt%) catalyst by co-precipitation method and applied it to CO catalytic oxidation. The Ag-Sn/CeO_2 (4%) catalyst showed more excellent CO catalytic performance (T_{100} = 100 °C). According to TEM images, smaller Ag nanoparticles were formed on Ag-Sn/CeO_2 (4%) catalyst. Yu et al. (2013) prepared Ag/Co_3O_4 catalyst by one-pot method (OP) and impregnation method (IM) and conducted CO catalytic oxidation test. Ag/Co_3O_4-OP had better CO catalytic efficiency than Ag/Co_3O_4-IM. According to the N_2 adsorption desorption curve, BJH pore size distribution curve, and XRD test results, it was found that the Ag/Co_3O_4-OP has a higher specific surface area, smaller pore size, and better dispersion of Ag nanoparticles than the Ag/Co_3O_4-IM. Zhang et al. (2017) loaded Ag nanoparticles on Pr_6O_{11} nanorods (Ag/Pr_6O_{11}-NRs) or nanoparticles (Ag/Pr_6O_{11}-NPs) through the impregnation method. The CO catalytic performance of Ag/Pr_6O_{11}-NRs (T_{100} = 210 °C) was better than Ag/Pr_6O_{11}-NPs (T_{100} = 320 °C). Zhang et al. (2016a, b) prepared Ag/Al-SBA-15, Ag/SiO_2, and Ag/Fe_2O_3 samples by different methods. The effect of different Si/Al ratios on the catalytic activity of CO was investigated on Ag/Al-SBA-15. The appropriate Si/Al ratio (200-50) was beneficial to the catalytic activity of CO. Overdoping with Al led to the formation of more Ag_2O species, making it less prone to CO catalytic oxidation. On the Ag/SiO_2 catalyst (Zhang et al. 2016a, b), the support was calcined at different temperatures (450–850 °C) for 5 h and then impregnated with Ag species. Among them, the catalyst heat-treated at 750 °C gave the highest Ag dispersion, resulting in the best activity of CO oxidation. The effect of different Fe/Ag atomic ratios on CO performance was investigated on Ag/Fe_2O_3 samples (Zhang et al. 2018). The catalyst with Fe/Ag ratio of 15 (Ag/Fe_2O_3-15) showed the best CO catalytic activity (T_{100} = 160 °C). In addition, adding 1% water vapor in the reaction atmosphere, the CO catalytic activity was suppressed.

Effect of physicochemical properties

Current researches demonstrated that the higher the dispersion degree of Ag nanoparticles on catalysts, the smaller the nanoparticle size, resulting in the higher CO catalytic oxidation activity. For example, the nanoclusters with the smallest particle size on the Ag/SiO_2 (Dutov et al. 2016) showed the best CO catalytic oxidation performance. In addition, metal Ag^0 species is the key factor to obtain high CO catalytic oxidation activity.

Reaction mechanisms

On the Ag/BN NHs catalyst (Konopatsky et al. 2018), the reaction mechanism of CO catalytic oxidation follows the L-H mechanism: The adsorbed oxygen atoms by O_2 dissociation react with the adsorbed CO to form CO_2. In addition, lattice oxygen on Ag/CeO_2 (Qu et al. 2013; Rao et al. 2020) provided as active oxygen species for CO catalytic oxidation, indicating that the reaction pathway of CO catalytic oxidation followed the typical MvK mechanism.

Other noble metal-based catalysts

Ru-based catalysts

The support plays an important role in the performance of CO oxidation for the Ru-based catalysts. Satsuma et al. (2013) physically mixed Ru metal powder (36 nm) with different supports (CeO_2, ZrO_2, MgO, Al_2O_3, TiO_2, SnO_2, and SiO_2), and calcined at 700 °C for 1 h, then reduced them at 400 °C with 5% H_2. The Ru–O–Ce bonds formed during the treatment process were beneficial to the dispersion of Ru nanoparticles. Therefore, the Ru+CeO_2 catalyst exhibited the highest CO catalytic oxidation activity. On Ru/graphene catalyst, it showed excellent CO oxidation activity at low temperature (Li et al. 2016) (T_{100} = 25 °C). Petrović et al. (2006) studied perovskite $La_{0.7}Sr_{0.3}Cr_{1-x}Ru_xO_3$ ($0.025 \le X \le 0.100$) catalysts with different Cr/Ru ratios and tested their CO oxidation activity. Among them, $La_{0.7}Sr_{0.3}Cr_{0.9}Ru_{0.1}O_3$ exhibited the highest CO catalytic activity (T_{50} = 140 °C). However, when X increased from 0.075 to 0.1, the performance CO oxidation of the samples increased very little. According to XPS characterization, it was found that $La_{0.7}Sr_{0.3}Cr_{1-x}Ru_xO_3$ ($0.075 \le X \le 0.100$) had almost the same Ru species on the sample surface. Li et al. (2019) used an impregnation method to load Ru onto CeO_2 nanorods (NR), nanotubes (NC), and nanoctahedra (NO) and conducted reduction treatment. Compared with the

5Ru/CeO_2 NC-r and 5Ru/CeO_2 NO-r, the strong metal-support interaction on the 5Ru/CeO_2 NR-r catalyst led to the formation of more oxygen vacancies on support, which was beneficial to anchor and disperse RuO_x nanoclusters. In addition, the XPS and DRIFTS results indicated that the strong metal-support interaction led to the formation of more Ru^{n+} species on the 5Ru/CeO_2 NR-r, and the Ru^{n+} species were more beneficial to activate CO. Therefore, the 5Ru/CeO_2 NR-r catalyst showed the highest performance of CO oxidation (T_{50} = 50 °C). The particle size of the active component nanoparticles and their valence are important factors that affect the performance of the catalyst for CO oxidation. On the 5Ru/CeO_2 NR-r catalyst, the high dispersion degree of Ru nanoclusters and the Ru^{n+} in the oxidation state seemed to be conducive to high CO catalytic performance. However, on the Ru film catalyst, the Ru species were oxidized and the CO catalytic activity was reduced. At high temperature (200 °C), the reduction treatment could only recover part of the activity. Furthermore, Qadir et al. (2013) reported that the catalyst with large Ru particles had better CO catalytic oxidation activity than the catalyst with small particles. According to the Ambient Pressure XPS (AP-XPS) results, it was found that the Ru species on the large particle were less oxidized than the small particle. These results showed that the metal Ru was easier to catalyze CO oxidation than the Ru species in the oxidation state.

Rh-based catalyst

Nishida et al. (2017) prepared Rh-PVP/γ-Al_2O_3 catalysts with controlled Rh nanoparticles (3.3–10.9 nm) by microblog-assisted alcohol reduction method for CO catalytic oxidation. Among them, the catalyst prepared by ethanol reduction has the smallest particle size and gave the best CO catalytic activity. In addition, according to TEM, XRD characterization, and CO activity tests, it was found that the activity of CO oxidation increased with the size of Rh nanoparticles reduced. McClure et al. (2009) oxidized the shell of Rh nanoparticles by UV/O_3 to improve the CO catalytic oxidation activity of the Rh catalyst. For Rh NP samples, the catalyst with UV/O_3 treated for 24 h still showed higher CO catalytic activity than the untreated catalyst. According to the results of XPS characterization and CO activity tests, the CO activity of Rh species in the oxidation state was higher than that in the metal state.

Experimental results and theoretical calculations on single-atom Rh_1/ZnO catalyst (Han et al. 2019) and Rh/phosphotungstic acid catalyst (Zhang et al. 2019a, b) proved that CO catalytic oxidation followed the MvK mechanism. In addition, on the Rh/Fe_2O_3 catalyst (Jakub et al. 2020), the CO catalytic oxidation followed the L-H mechanism when the temperature was below − 73 °C, but when the temperature was 27 °C, CO was excessively adsorbed on the Rh sites; therefore, CO catalytic oxidation followed the MvK mechanism.

Ir-based catalyst

Lin et al. (2011) studied the adsorption and reaction behavior of CO on Ir-in-CeO_2 and Ir-on-CeO_2 catalysts by in situ calorimetric method. Ir-in-CeO_2 and Ir-on-CeO_2 catalysts were prepared by co-precipitation method and DP method, respectively. According to UV-Raman characterization results, there were more oxygen vacancies on Ir-in-CeO_2, which led to more carbonate species accumulation on the surface of the catalyst. However, the presence of more Ru sites on the Ir-on-CeO_2 catalyst was beneficial for CO adsorption. In addition, the Ir-in-CeO_2 catalyst (Lin et al. 2012) has been investigated in depth for an optimal oxygen vacancy of 1.5%. The catalytic activity for CO oxidation of the single-atom Pt/FeO_x was better than Ir/FeO_x, which was consistent with the DFT calculation results (Liang et al. 2014). Okumura et al. (2002) used the DP method to support Ir on different carries (SnO_2, Al_2O_3, Fe_2O_3, and TiO_2) for CO catalytic oxidation research, of which Ir/TiO_2 gave the highest CO catalytic performance. In addition, the effect of different PH (PH = 3, 5, 7, 8, and 10) during the preparation process on the catalytic oxidation of CO over Ir/TiO_2 catalyst was also investigated. According to the ICP results, when the PH = 8, the loading of Ir on the Ir/TiO_2 catalyst was the largest so the performance of CO oxidation was the best after reduction treatment. Zhang et al. (2015) prepared Ir/FeO_x-CA and Ir/FeO_x-PM catalysts by citric acid sol-gel method and precipitation method, respectively. Among them, Ir/FeO_x-CA catalyst gave the best catalytic activity for CO oxidation. The results of XRD characterization indicated that metal Fe existed at the metal interface of Ir/FeO_x-PM, which led to inhibit the supply of active oxygen species required for CO catalytic oxidation.

There was no CO catalytic activity over the non-reduced Ir/TiO_2 at low temperature. The Ir/TiO_2 catalyst exhibited CO catalytic activity at 40 °C after reduction treatment, which showed that the metal Ir has a higher catalytic oxidation activity than the oxidized Ir at low temperature (Okumura et al. 2002).

It was proposed that the reaction of CO catalytic oxidation follows the L-H mechanism over Ir-on-CeO_2. On the single-atom Ir/FeO_x catalyst, Liang et al. (2014) also proposed that the pathway of CO catalytic oxidation followed the L-H mechanism. On the single-atom Ir-on-$MgAl_2O_4$ catalyst, Lu et al. (2018) proposed that CO oxidation followed the E-R mechanism based on kinetic tests and DFT calculations. Performance of some typical noble metal catalysts for the catalytic oxidation of CO is summarized in Table 1.

Table 1 Activity of various noble metal catalysts for CO catalytic oxidation

Catalysts	Reaction conditions					CO conversion (%)	Temperature (°C)	References
	Temperature range (°C)	GHSV[a] or WHSV[b]	CO concentration (ppm)	O_2 content (%)	Other gases			
2%Pt/$MgFe_2O_3$	20–80	60000 mL g^{-1} h^{-1}	10000	5	/	100	20	Zheng et al. (2016)
2%Pt/CeO_2	150–270	120000 h^{-1}	1000	10	/	90	149	(Lee et al. 2018a, b)
0.8%Pt/TiO_2-001	40–200	360000 h^{-1}	1000	2.5	/	50	191	Zhou et al. (2016)
1.1%Pt/TiO_2-101	40–200	360000 h^{-1}	1000	2.5	/	50	92	Zhou et al. (2016)
1.2%Pt/TiO_2-110	40–200	360000 h^{-1}	1000	2.5	/	50	98	Zhou et al. (2016)
2.5%Pt/DBD-WO_3	20–200		10000	20	/	100	145	Wang et al. (2014)
2.5%Pt/c-WO_3	20–200		10000	20	/	100	180	Wang et al. (2014)
0.8%Pt/MnO_x	60–200		10000	1	/	100	100	Zhang et al. (2016)
Pt/Fe_2O_3	20–90	9600 h^{-1}	5000	10	/	42	35	An et al. (2013a, b)
4%Pt/SiO_2	120–280	15000 h^{-1}	40000	10	/	100	180	Jung et al. (2014)
Pt-Sn/SiO_2	0–150	30000 mL g^{-1} h^{-1}	21000	5.9	/	50	25	Margitfalvi and Irina (2002)
0.42%K-2%Pt/Al_2O_3	120–280	9600 h^{-1}	10000	1	/	100	180	Liu et al. (2015)
1%Pt/TiO_2-Co	20–140	30000 mL g^{-1} h^{-1}	10000	20	/	100	70	Zhao et al. (2018)
1%Pt/TiO_2 (R)-600	25	120000 h^{-1}	1500	21	/	12.4	25	Kim et al. (2016)
1%Pt/TiO_2 (B)	80–160	22500 mL g^{-1} h^{-1}	9000	24	/	100	120	Liu et al. (2018a, b)
2%Pt/$Cr_{1.3}Fe_{0.7}O_3$	50–200	120000 mL g^{-1} h^{-1}	10000	1	/	78.8	80	Wang et al. (2019)
2%Pt/$Cr_{1.3}Fe_{0.7}O_3$	50–200	120000 mL g^{-1} h^{-1}	10000	1	10% CO_2	48	80	Wang et al. (2019)
2%Pt/$Cr_{1.3}Fe_{0.7}O_3$	50–200	120000 mL g^{-1} h^{-1}	10000	1	10% H_2O + 10% CO_2	100	80	Wang et al. (2019)
0.2%Pt/$Cr_{1.3}Fe_{0.7}O_3$	40–220	120000 mL g^{-1} h^{-1}	10000	1	/	14.2	80	Wang et al. (2020)
0.2%Pt/$Cr_{1.3}Fe_{0.7}O_3$	40–220	120000 mL g^{-1} h^{-1}	10000	1	10% H_2O	92.4	80	Wang et al. (2020)
0.2%Pt/$Cr_{1.3}Fe_{0.7}O_3$	40–220	120000 mL g^{-1} h^{-1}	10000	1	10% H_2O + 10% CO_2	64	80	Wang et al. (2020)
Pt/TiO_2	250	600000 mL g^{-1} h^{-1}	10000	10	20% H_2O + 40 ppm SO_2	60	250	Taira et al. (2016)
Pt_1/CeO_2	20–180	18000 mL g^{-1} h^{-1}	10000	20	/	100	160	Wang et al. (2016)
Pt_1/CeO_2	20–180	18000 mL g^{-1} h^{-1}	10000	20	0.04% H_2O	100	100	Wang et al. (2016)
3.8%Au/ZnO	− 103–97	20000 mL g^{-1} h^{-1}	10000	20	/	90	− 50	Fujita et al. (2019)
1%Au/La-P-O-NW	0–100	18000 mL g^{-1} h^{-1}	10000	20	/	100	15	Liu et al. (2016)
2.4%Au/$SrTiO_3$	0–200	20000 mL g^{-1} h^{-1}	10000	20	/	100	50	Akita and Maeda (2018)
1%Au/$Ni_{0.05}Al$	− 25–200	80400 mL g^{-1} h^{-1}	10000	20	/	100	20	Lu et al. (2020)
Au/$CeZrLaO_x$	0–200	80400 mL g^{-1} h^{-1}	10000	20	/	100	140	Yang et al. (2016)
1%Au/TiO_2	− 100–200	19800 mL g^{-1} h^{-1}	10000	20	/	100	0	Rutha et al. (2000)
1%Au/TiO_2	− 100–200	19800 mL g^{-1} h^{-1}	10000	20	500 ppm SO_2	100	150	Rutha et al. (2000)
0.92%Au/TiO_2	25–300	30000 mL g^{-1} h^{-1}	10000	20	/	100	25	Kim et al. (2006)
0.92%Au/TiO_2	25–250	60000 mL g^{-1} h^{-1}	10000	20	5000 ppm SO_2 pretreated at rt[d] for 1 h	100	150	Kim et al. (2006)
1%Au/La_2O_3/TiO_2	200–600	5000 h^{-1}	16000	4.1	13.2% CO_2 + 22% H_2O + 1% H_2S + 0.2% SO_2 + 0.05% COS +0.02% CS_2	99.3	300	Clark et al. (2013)
1%Au/Eu_2O_3/TiO_2	200–350	5000 h^{-1}	10300	5.2	1.29% H_2 + 0.64% H_2S + 0.29% SO_2 + 16.74% H_2O + 14.94% CO_2	96.1	300	Kazemi et al. (2019)
4%Pd/Mn_3O_4	0–125	60000 mL g^{-1} h^{-1}	4[c]	20[c]	/	100	20	Khder et al. (2019)

Table 1 (continued)

Catalysts	Reaction conditions					CO conversion (%)	Temperature (°C)	References
	Temperature range (°C)	GHSV[a] or WHSV[b]	CO concentration (ppm)	O_2 content (%)	Other gases			
0.93%Pd/TiO_2	40–180	30000 mL g^{-1} h^{-1}	10000	20	/	100	80	Zhai et al. (2018)
Pd/γ-Fe_2O_3-R	− 40–300	15000 mL g^{-1} h^{-1}	10000	20	/	100	0	Wang et al. (2017a, b)
1.5%Pd/CoO_x-InO_x-500	10–100	10000 mL g^{-1} h^{-1}	10000	20	/	50	52	Du et al. (2019)
5%Pd/Co_3O_4-200	30–240	120000 mL g^{-1} h^{-1}	10000	1	/	50	113.9	Huang et al. (2019)
1%Pd/PCZA	50–250	240000 mL g^{-1} h^{-1}	1000	9.5	/	50	60	Shi et al. (2017)
1%S-Pd/SGCZA	50–250	240000 mL g^{-1} h^{-1}	1000	9.5	250 ppm SO_2 pretreated at 300 °C for 3 h	50	123	Shi et al. (2017)
1%Pd/SMC	0–500	40000 h^{-1}	20000	5	/	70	50	Wang et al. (2015)
2.5%Pd/La-Al_2O_3	30–250	22500 mL g^{-1} h^{-1}	19000	1	/	50	197	Gaudet et al. (2013)
$Ti_{0.97}Pd_{0.03}O_{2-x}$	20–130	47770 h^{-1}	10000	1	/	100	60	Mukri et al. (2012)
7%Ag/ZSM-5	20–160	12000 mL g^{-1} h^{-1}	50000	5	/	90	40	Kolobova et al. (2017)
5%Ag/SiO_2-900	− 50–300	12000 mL g^{-1} h^{-1}	10000	1	/	98	50	Dutov et al. (2016)
7Ag/KCC-1	30–260	18000 mL g^{-1} h^{-1}	10000	21	/	100	120	Xu et al. (2017)
10%Ag/CeO_2	− 50–450	40000 mL g^{-1} h^{-1}	5000	4.4	/	50	99	Grabchenko et al. (2020)
8%Ag/CeO_2	25–400	9000 mL g^{-1} h^{-1}	10000	20	/	100	65	Qu et al. (2013)
1.36%Ag/BN	175–350	25000 mL g^{-1} h^{-1}	40000	16	/	100	195	Konopatsky et al. (2018)
4.5%Ag/$Ce_{0.67}Zr_{0.33}O_2$	150–550	0.06 g s mL^{-1}	5000	5	/	50	282	Lee et al. (2018a, b)
8%Ag/Co_2O_3	-	9000 mL g^{-1} h^{-1}	10000	20	/	100	− 10–20	Yu et al. (2013)
8%Ag/Al-SBA-15	20–220	9000 mL g^{-1} h^{-1}	10000	20	/	100	40	Zhang et al. (2015)
4%Ag/SiO_2	20–260	9000 mL g^{-1} h^{-1}	10000	20	/	98	105	Zhang et al. (2016a, b)
3.41Ag/Fe_2O_3	100–260	18000 mL g^{-1} h^{-1}	10000	20	/	100	160	Zhang et al. (2018)
2%Ru+CeO_2	0–300	600000 mL g^{-1} h^{-1}	4000	10		100	180	Satsuma et al. (2013)
0.01%Rh_1/ZnO	150–400	40000 mL g^{-1} h^{-1}	10000	1	/	100	210	Han et al. (2019)
0.22%Ir_1/FeO_x	20–120	18000 mL g^{-1} h^{-1}	10000	1	40% H_2	100	40	Zhang et al. (2015)

[a] GHSV means gaseous hourly space velocity (h^{-1})

[b] WHSV means weight hourly space velocity (mL g^{-1} h^{-1} or g s mL^{-1})

[c] The percentage of mass (wt.%)

[d] rt means room temperature

Conclusions

This article reviewed the noble metal catalysts for CO catalytic oxidation. The CO oxidation on the reducible carrier-supported catalyst follows the MvK mechanism, avoiding the deactivation caused by excessive CO adsorption on the metal sites. Therefore, the reducible carrier-supported noble metal catalyst exhibits better low-temperature CO catalytic oxidation activity than the non-reducible carrier-supported noble metal catalyst. H_2 reduction treatment adjusts the interaction between the metal and support to obtain a high degree of dispersion of the active components. Moreover, the active components (Pt, Au, Pd, Ag, Ir, Ru) in the ionic state are reduced to the metal state during the reduction process, resulting in high CO oxidation activity of the catalyst at low temperature. On Rh-based catalysts, it seems that Rh species in the oxidized state are more advantageous to the activation of the reactants. It is a feasible strategy to improve the low-temperature catalytic oxidation of CO by doping noble metal catalysts. When only water vapor exists in the simulated reaction atmosphere, the reaction pathway of CO catalytic oxidation on the Pt, Au-based catalysts is changed. Previous studies found that the water vapor dissociates into -OH groups as active oxygen species to participate in the CO catalytic oxidation reaction. Besides, the liquid hydrolysis dissociated into OH^- or H^+ promoting the activation of oxygen or accelerating the decomposition of intermediate products.

Taira's group (Taira et al. 2016; Taira and Einaga 2019) found that Pt/TiO_2 catalyst exhibited excellent CO catalytic oxidation activity with low Pt loading (0.1%) at 250 °C and extremely high space velocity. Especially when the reaction atmosphere contains 20% water vapor, the catalytic oxidation of CO was greatly promoted demonstrating that Pt-based catalysts have great potential for CO purification of industrial flue gas. At present, the main reasons why noble metal catalysts are difficult to use for CO catalytic oxidation purification in actual industrial flue gas are as follows: (1) The high price of noble metals limits its loading on the catalyst. (2) The composition of industrial flue gas is very complex, especially containing a large amount of water vapor and a small amount of SO_2, which leads to catalyst poisoning and deactivation. In the future, it is very necessary to develop low loading noble metal catalysts with high CO catalytic oxidation activity under complex reaction atmosphere conditions at 100–250 °C. Based on our summary here, this review will facilitate the future development and application of noble metal catalysts to purify CO in industrial flue gas.

Acknowledgements We thank Mr. Hu for valuable discussions.

Availability of data and materials Not applicable.

Author contribution Chenglin Feng: writing - original Draft, visualization, data curation, conceptualization

Xiaolong Liu: conceptualization, writing - review and editing, supervision, project administration, funding acquisition

Tingyu Zhu: writing - review and editing, supervision, project administration, funding acquisition

Mengkui Tian: visualization

Funding This work was supported by National Key Research and Development Program of China (2018YFC0213400) and National Natural Science Foundation of China (51938014).

Declarations

Ethics approval and consent to participate Not applicable.

Consent for publication Not applicable.

Competing interests The authors declare no competing interests.

References

Afanasev DS, Yakovina OA, Kuznetsova NI, Lisitsyn AS (2012) High activity in CO oxidation of Ag nanoparticles supported on fumed silica. Catal Commun 22:43–47. https://doi.org/10.1016/j.catcom.2012.02.014

Akita T, Maeda Y (2018) CO oxidation properties and scanning transmission electron microscopy observation of $Au/SrTiO_3$ catalysts. Catal Lett 148:3035–3041. https://doi.org/10.1007/s10562-018-2505-2

Allian AD, Takanabe K, Fujdala KL, Hao X, Truex TJ, Cai J, Buda C, Neurock M, Iglesia E (2011) Chemisorption of CO and mechanism of CO oxidation on supported platinum nanoclusters. J Am Chem Soc 133:4498–4517. https://doi.org/10.1021/ja110073u

An K, Alayoglu S, Musselwhite N, Plamthottam S, Melaet G, Lindeman AE, Lindeman AE, Somorjai GA (2013a) Enhanced CO oxidation rates at the interface of mesoporous oxides and Pt nanoparticles. J Am Chem Soc 135:16689–16696. https://doi.org/10.1021/ja4088743

An N, Li S, Duchesne PN, Wu P, Zhang W, Lee JF, Cheng S, Zhang P, Jia M, Zhang W (2013b) Size effects of platinum colloid particles on the structure and CO oxidation properties of supported Pt/Fe_2O_3 catalysts. J Phys Chem C 117:21254–21262. https://doi.org/10.1021/jp404266p

Bond G, Thompson D (2001) Gold-catalysed oxidation of carbon monoxide. Gold Bull 33:41–51. https://doi.org/10.1007/BF03216579

Bond G, Thompson D (2009) Formulation of mechanisms for gold-catalysed reactions. Gold Bull 42:247–259. https://doi.org/10.1007/BF03214946

Bourane A (2004) Oxidation of CO on a Pt/Al_2O_3 catalyst: from the surface elementary steps to light-off tests V. Experimental and kinetic model for light-off tests in excess of O_2. J Catal 222:499–510. https://doi.org/10.1016/j.jcat.2003.11.019

Cai J, Zhang J, Cao K, Gong M, Lang Y, Liu X, Chu S, Shan B, Chen R (2018) Selective passivation of Pt nanoparticles with enhanced sintering resistance and activity toward CO oxidation via atomic layer deposition. ACS Appl Nano Mater 1:522–530. https://doi.org/10.1021/acsanm.7b00026

Carabineiro SAC, Silva AMT, Drazic G, Tavares PB, Figueiredo JL (2010) Effect of chloride on the sinterization of Au/CeO_2 catalysts. Catal Today 154:293–302. https://doi.org/10.1016/j.cattod.2009.12.017

Carrettin S, Hao Y, Aguilar-Guerrero V, Gates BC, Trasobares S, Calvino JJ et al (2007) Increasing the number of oxygen vacancies on TiO_2

by doping with iron increases the activity of supported gold for CO oxidation. Chem 13:7771–7779. https://doi.org/10.1002/chem.200700472

Clark PD, Sui R, Dowling NI, Huang M, Lo JMH (2013) Oxidation of CO in the presence of SO_2 using gold supported on La_2O_3/TiO_2 nanofibers. Catal Today 207:212–219. https://doi.org/10.1016/j.cattod.2012.05.033

Comotti M, Li W-C, Spliethoff B, Schüth F (2006) Support effect in high activity gold catalysts for CO oxidation. J Am Chem Soc 128:917–924

Date M, Okumura M, Tsubota S, Haruta M (2004) Vital role of moisture in the catalytic activity of supported gold nanoparticles. Angew Chem Int Ed Eng 43:2129–2132. https://doi.org/10.1002/anie.200453796

Du X, Han W, Tang Z, Zhang J (2019) Controlled synthesis of Pd/CoO_x–InO_x nanofibers for low-temperature CO oxidation reaction. New J Chem 43:14872–14882. https://doi.org/10.1039/C9NJ03055G

Duan Z, Henkelman G (2018) Calculations of CO oxidation over a Au/TiO_2 catalyst: a study of active sites, catalyst deactivation, and moisture effects. ACS Catal 8:1376–1383. https://doi.org/10.1021/acscatal.7b03993

Dutov VV, Mamontov GV, Zaikovskii VI, Vodyankina OV (2016) The effect of support pretreatment on activity of Ag/SiO_2 catalysts in low-temperature CO oxidation. Catal Today 278:150–156. https://doi.org/10.1016/j.cattod.2016.05.033

Fujita T, Ishida T, Shibamoto K, Honma T, Ohashi H, Murayama T, Haruta M (2019) CO oxidation over Au/ZnO: unprecedented change of the reaction mechanism at low temperature caused by a different O_2 activation process. ACS Catal 9:8364–8372. https://doi.org/10.1021/acscatal.9b02128

Ganzler AM, Casapu M, Doronkin DE, Maurer F, Lott P, Glatzel P et al (2019) Unravelling the different reaction pathways for low temperature CO oxidation on Pt/CeO_2 and Pt/Al_2O_3 by spatially resolved structure-activity correlations. J Phys Chem Lett 10:7698–7705. https://doi.org/10.1021/acs.jpclett.9b02768

Gaudet JR, de la Riva A, Peterson EJ, Bolin T, Datye AK (2013) Improved low-temperature CO oxidation performance of Pd supported on La-stabilized alumina. ACS Catal 3:846–855. https://doi.org/10.1021/cs400024u

Gogate MR (2019) Catalysis by nanoscale gold (Au/MO_x): Reaction mechanisms of low temperature CO oxidation reactions. Pet Sci Technol 37:1208–1215. https://doi.org/10.1080/10916466.2019.1587460

Grabchenko MV, Mamontov GV, Zaikovskii VI, La Parola V, Liotta LF, Vodyankina OV (2020) The role of metal–support interaction in Ag/CeO_2 catalysts for CO and soot oxidation. Appl Catal B Environ 260:118–148. https://doi.org/10.1016/j.apcatb.2019.118148

Green IX, Tang WJ, Neurock M, Yates JT (2011) Spectroscopic observation of dual catalytic sites during oxidation of CO on a Au/TiO_2 catalyst. Science 33:736–739. https://doi.org/10.1126/science.1207272

Guo J, Han Q, Zhong S, Zhu B, Huang W, Zhang S (2018) Au/M-TiO_2 nanotube catalysts (M = Ce, Ga, Co, Y): preparation, characterization and their catalytic activity for CO oxidation. J Sol-Gel Sci Techn 86:699–710. https://doi.org/10.1007/s10971-018-4691-1

Ha H, Yoon S, An K, Kim HY (2018) Catalytic CO oxidation over Au nanoparticles supported on CeO_2 nanocrystals: effect of the Au–CeO_2 interface. ACS Catal 8:11491–11501. https://doi.org/10.1021/acscatal.8b03539

Han B, Lang R, Tang H, Xu J, Gu XK, Qiao B, Liu J(J) (2019) Superior activity of Rh_1/ZnO single-atom catalyst for CO oxidation. Chin J Catal 40:1847–1853. https://doi.org/10.1016/S1872-2067(19)63411-X

Haruta M (2011) Role of perimeter interfaces in catalysis by gold nanoparticles. Faraday Discuss 152:11–32. https://doi.org/10.1039/C1FD00107H

Haruta M, Kobayashi T, Sano H, Yamada N (1987) Novel gold catalysts for the oxidation of carbon monoxide at a temperature far below 0 °C. Chem Lett 2:405–408. https://doi.org/10.1246/cl.1987.405

Haruta M, Tsubota S, Kobayashi T, Kageyama H, Genet MJ, Delmon B (1993) Low-temperature oxidation of CO over gold supported on TiO_2, Alpha-Fe_2O_3, and Co_3O_4. J Catal 144:175–192. https://doi.org/10.1006/jcat.1993.1322

Huang R, Kim K, Kim HJ, Jang MG, Han JW (2019) Size-controlled Pd nanoparticles loaded on Co_3O_4 nanoparticles by calcination for enhanced CO oxidation. ACS Appl Nano Mater 3:486–495. https://doi.org/10.1021/acsanm.9b02056

Ishida T, Murayama T, Taketoshi A, Haruta M (2020) Importance of size and contact structure of gold nanoparticles for the genesis of unique catalytic processes. Chem Rev 120:464–525. https://doi.org/10.1021/acs.chemrev.9b00551

Jain D, Madras G (2017) Mechanistic insights and kinetics of CO oxidation over pristine and noble metal modified Fe_2O_3 using diffuse reflectance infrared Fourier transform spectroscopy. Ind Eng Chem Res 56:2008–2024. https://doi.org/10.1021/acs.iecr.6b04856

Jakub Z, Hulva J, Ryan PTP, Duncan DA, Payne DJ, Bliem R, Ulreich M, Hofegger P, Kraushofer F, Meier M, Schmid M, Diebold U, Parkinson GS (2020) Adsorbate-induced structural evolution changes the mechanism of CO oxidation on a $Rh/Fe_3O_4(001)$ model catalyst. Nanoscale. 12:5866–5875. https://doi.org/10.1039/C9NR10087C

Jeong H, Bae J, Han JW, Lee H (2017) Promoting effects of hydrothermal treatment on the activity and durability of Pd/CeO_2 catalysts for CO oxidation. ACS Catal 7:7097–7105. https://doi.org/10.1021/acscatal.7b01810

Jung CH, Yun J, Qadir K, Naik B, Yun JY, Park JY (2014) Catalytic activity of Pt/SiO_2 nanocatalysts synthesized via ultrasonic spray pyrolysis process under CO oxidation. Appl Catal B Environ 154-155:171–176. https://doi.org/10.1016/j.apcatb.2014.02.014

Kazemi ML, Sui R, Clark PD, Marriott RA (2019) Catalytic combustion of Claus tail gas: oxidation of sulfur species and CO using gold supported on lanthanide-modified TiO_2. Appl Catal A Gen 587:117–256. https://doi.org/10.1016/j.apcata.2019.117256

Khan IA, Sajid N, Badshah A, Wattoo MHS, Anjum DH, Nadeem MA (2015) CO oxidation catalyzed by Ag nanoparticles supported on SnO/CeO_2. J Braz Chem Soc 26:695–704. https://doi.org/10.5935/0103-5053.20150028

Khder AERS, Altass HM, Orif MI, Ashour SS, Almazroai LS (2019) Preparation and characterization of highly active Pd nanoparticles supported Mn_3O_4 catalyst for low-temperature CO oxidation. Mater Res Bull 113:215–222. https://doi.org/10.1016/j.materresbull.2019.02.011

Kim MR, Woo SI (2006) Poisoning effect of SO_2 on the catalytic activity of Au/TiO_2 investigated with XPS and in situ FT-IR. Appl Catal A Gen 299:52–57. https://doi.org/10.1016/j.apcata.2005.10.030

Kim TS, Gong JL, Ojifinni RA, White JM, Mullins CB (2006) Water activated by atomic oxygen on Au(111) to oxidize CO at low temperatures. J Am Chem Soc 128:6282–6283. https://doi.org/10.1021/ja058263m

Kim GJ, Kwon DW, Hong SC (2016) Effect of Pt particle size and valence state on the performance of Pt/TiO_2 catalysts for CO oxidation at room temperature. J Phys Chem C 120:17996–18004. https://doi.org/10.1021/acs.jpcc.6b02945

Kolobova E, Pestryakov A, Mamontov G, Kotolevich Y, Bogdanchikova N, Farias M, Vosmerikov A, Vosmerikova L, Cortes Corberan V (2017) Low-temperature CO oxidation on Ag/ZSM-5 catalysts: influence of Si/Al ratio and redox pretreatments on formation of silver active sites. Fuel 188:121–131. https://doi.org/10.1016/j.fuel.2016.10.037

Konopatsky AS, Leybo DV, Firestein KL, Popov ZI, Bondarev AV, Manakhov AM, Permyakova ES, Shtansky DV, Golberg DV (2018) Synthetic routes, structure and catalytic activity of Ag/BN

nanoparticle hybrids toward CO oxidation reaction. J Catal 368: 217–227. https://doi.org/10.1016/j.jcat.2018.10.016

Lee C, Jeon Y, Kim T, Tou A, Park JI, Einaga H, Shul YG (2018a) Ag-loaded cerium-zirconium solid solution oxide nano-fibrous webs and their catalytic activity for soot and CO oxidation. Fuel 212: 395–404. https://doi.org/10.1016/j.fuel.2017.10.007

Lee J, Ryou Y, Kim J, Chan X, Kim TJ, Kim DH (2018b) Influence of the defect concentration of ceria on the Pt dispersion and the CO oxidation activity of Pt/CeO_2. J Phys Chem C 122:4972–4983. https://doi.org/10.1021/acs.jpcc.8b00254

Li W, Zhang H, Wang J, Qiao W, Ling L, Long D (2016) Flexible Ru/graphene aerogel with switchable surface chemistry: highly efficient catalyst for room-temperature CO oxidation. Adv Mater Interfaces 3:1500711. https://doi.org/10.1002/admi.201500711

Li JJ, Zhu BL, Wang GC, Liu ZF, Huang WP, Zhang SM (2018) Enhanced CO catalytic oxidation over an Au–Pt alloy supported on TiO nanotubes: investigation of the hydroxyl and Au/Pt ratio influences. Catal Sci Technol 8:6109–6122. https://doi.org/10.1039/c8cy01642a

Li J, Liu Z, Cullen DA, Hu W, Huang J, Yao L, Peng Z, Liao P, Wang R (2019) Distribution and valence state of Ru species on CeO_2 supports: support shape effect and its influence on CO oxidation. ACS Catal 9:11088–11103. https://doi.org/10.1021/acscatal.9b03113

Li H, Shen M, Wang J, Wang H, Wang J (2020) Effect of support on CO oxidation performance over the Pd/CeO_2 and Pd/CeO_2–ZrO_2 catalyst. Ind Eng Chem Res 59:1477–1486. https://doi.org/10.1021/acs.iecr.9b05351

Liang JX, Lin J, Yang XF, Wang A-Q, Qiao BT, Liu J, Zhang T, Li J (2014) Theoretical and experimental investigations on single-atom catalysis: Ir_1/FeO_x for CO oxidation. J Phys Chem C 118:21945–21951. https://doi.org/10.1021/jp503769d

Lin J, Li L, Huang Y, Zhang W, Wang X, Wang A, Zhang T (2011) In situ calorimetric study: structural effects on adsorption and catalytic performances for CO oxidation over Ir-in-CeO_2 and Ir-on-CeO_2 catalysts. J Phys Chem C 115:16509–16517. https://doi.org/10.1021/jp204288h

Lin J, Huang Y, Li L, Wang A, Zhang W, Wang X, Zhang T (2012) Activation of an Ir-in-CeO_2 catalyst by pulses of CO: the role of oxygen vacancy and carbonates in CO oxidation. Catal Today 180: 155–160. https://doi.org/10.1016/j.cattod.2011.03.066

Liu LM, McAllister B, Ye HQ, Hu P (2006) Identifying an O_2 supply pathway in CO oxidation on Au/TiO_2(110): a density functional theory study on the intrinsic role of water. J Am Chem Soc 128: 4017–4022. https://doi.org/10.1021/ja056801p

Liu H, Jia A, Yu W, Luo M, Lu J (2015) Enhanced CO oxidation over potassium-promoted Pt/Al_2O_3 catalysts: kinetic and infrared spectroscopic study. Chin J Catal 36:1976–1986. https://doi.org/10.1016/S1872-2067(15)60950-0

Liu H, Lin Y, Ma Z (2016) Au/$LaPO_4$ nanowires: synthesis, characterization, and catalytic CO oxidation. J Taiwan Inst Chem E 62:275–282. https://doi.org/10.1016/j.jtice.2016.01.016

Liu J, Ding T, Zhang H, Li G, Cai J, Zhao D, Tian Y, Xian H, Bai X, Li X (2018a) Engineering surface defects and metal–support interactions on Pt/TiO_2(B) nanobelts to boost the catalytic oxidation of CO. Catal Sci Technol 8:4934–4944. https://doi.org/10.1039/C8CY01410H

Liu SP, Zhao M, Sun GE, Gao W, Jiang Q (2018b) Different effects of water molecules on CO oxidation with different reaction mechanisms. Phys ChemChem Phys 20:8341–8348. https://doi.org/10.1039/C8CP00035B

Lou Y, Liu J (2017) CO oxidation on metal oxide supported single Pt atoms: the role of the support. Ind Eng Chem Res 56:6916–6925. https://doi.org/10.1021/acs.iecr.7b01477

Lu R, He L, Wang Y, Gao XQ, Li WC (2020) Promotion effects of nickel-doped Al_2O_3-nanosheet-supported Au catalysts for CO oxidation. Chinese J Catal 41:350–356. https://doi.org/10.1016/S1872-2067(19)63439-X

Lu Y, Wang J, Yu L, Kovarik L, Zhang X, Hoffman AS, Gallo A, Bare SR, Sokaras D, Kroll T, Dagle V, Xin H, Karim AM (2018) Identification of the active complex for CO oxidation over single-atom Ir-on-$MgAl_2O_4$ catalysts. Nat Catal 2:149–156. https://doi.org/10.1038/s41929-018-0192-4

Ma Z, Overbury SH, Dai S (2007) Au/M_xO_y/TiO_2 catalysts for CO oxidation: promotional effect of main-group, transition, and rare-earth metal oxide additives. J Mol Catal A Chem 273:186–197. https://doi.org/10.1016/j.molcata.2007.04.007

Mao X, Foucher A, Stach EA, Gorte RJ (2019) A study of support effects for CH_4 and CO oxidation over Pd catalysts on ALD-modified Al_2O_3. Catal Lett 149:905–915. https://doi.org/10.1007/s10562-019-02699-6

Margitfalvi JL, Irina B (2002) Low temperature oxidation of CO over tin-modified Pt/SiO_2 catalysts. Catal Today 73:343–353. https://doi.org/10.1016/S0920-5861(02)00018-4

McClure SM, Lundwall M, Yang F, Zhou Z, Goodman DW (2009) CO Oxidation on Rh/SiO2/Mo(112) Model Catalysts at Elevated Pressures. J Phys Chem C 113:9688–9697. https://doi.org/10.1021/jp808953v

Moses-DeBusk M, Yoon M, Allard LF, Mullins DR, Wu Z, Yang X, Veith G, Stocks GM, Narula CK (2013) CO oxidation on supported single Pt atoms: experimental and ab initio density functional studies of CO interaction with Pt atom on theta-Al_2O_3(010) surface. J Am Chem Soc 135:12634–12645. https://doi.org/10.1021/ja401847c

Mowery DL, McCormick RL (2001) Deactivation of alumina supported and unsupported PdO methane oxidation catalyst: the effect of water on sulfate poisoning. Appl Catal B Environ 34:287–297. https://doi.org/10.1016/S0926-3373(01)00222-3

Mukri BD, Dutta G, Waghmare UV, Hegde MS (2012) Activation of lattice oxygen of TiO_2 by Pd^{2+} ion: correlation of low-temperature CO and hydrocarbon oxidation with structure of $Ti_{1-x}Pd_xO_2$–x (x = 0.01–0.03). Chem Mater 24:4491–4502. https://doi.org/10.1021/cm301704u

Nakamura I, Fujitani T (2014) Effect of water on low-temperature CO oxidation over a Au/Al_2O_3 model catalyst. Catal Lett 144:1113–1117. https://doi.org/10.1007/s10562-014-1261-1

Nishida Y, Sato K, Yamamoto T, Wu D, Kusada K, Kobayashi H, Matsumura S, Kitagawa H, Nagaoka K (2017) Facile synthesis of size-controlled Rh nanoparticles via microwave-assisted alcohol reduction and their catalysis of CO oxidation. Chem Lett 46:1254–1257. https://doi.org/10.1246/cl.170440

Okumura M, Masuyama N, Konishi E, Ichikawa S, Akita T (2002) CO oxidation below room temperature over Ir/TiO_2 catalyst prepared by deposition precipitation method. J Catal 208:485–489. https://doi.org/10.1006/jcat.2002.3603

Panagiotopoulou P, Verykios XE (2017) Mechanistic study of the selective methanation of CO over Ru/TiO_2 catalysts: effect of metal crystallite size on the nature of active surface species and reaction pathways. J Phys Chem C 121:5058–5068. https://doi.org/10.1021/acs.jpcc.6b12091

Petrović S, Rakić V, Jovanović DM, Baričević AT (2006) Oxidation of CO over Ru containing perovskite type oxides. Appl Catal B Environ 66:249–257. https://doi.org/10.1016/j.apcatb.2006.04.003

Prasad R, Singh P (2012) A review on CO oxidation over copper chromite catalyst. Catal Rev 54:224–279. https://doi.org/10.1080/01614940.2012.648494

Qadir K, Kim SM, Seo H, Mun BS, Akgul FA, Liu Z, Park JY (2013) Deactivation of Ru catalysts under catalytic CO oxidation by formation of bulk Ru oxide probed with ambient pressure XPS. J Phys Chem C 117:13108–13113. https://doi.org/10.1021/jp402688a

Qiao B, Wang A, Yang X, Allard LF, Jiang Z, Cui Y, Liu J, Li J, Zhang T (2011) Single-atom catalysis of CO oxidation using Pt_1/FeO_x. Nat Chem 3:634–641. https://doi.org/10.1038/nchem.1095

Qu Z, Yu F, Zhang X, Wang Y, Gao J (2013) Support effects on the structure and catalytic activity of mesoporous Ag/CeO_2 catalysts for CO oxidation. Chem Eng J 229:522–532. https://doi.org/10.1016/j.cej.2013.06.061

Rao R, Shao F, Dong X, Dong H, Fang S, Sun H, Ling Q (2020) Effect of Ag-CeO_2 interface formation during one-spot synthesis of Ag-CeO_2 composites to improve their catalytic performance for CO oxidation. Appl Surf Sci 513:145–771. https://doi.org/10.1016/j.apsusc.2020.145771

Rodriguez JA, Grinter DC, Ramírez PJ, Stacchiola DJ, Senanayake S (2018) High activity of Au/K/TiO_2(110) for CO oxidation: alkali-metal-enhanced dispersion of Au and bonding of CO. J Phys Chem C 122:4324–4330. https://doi.org/10.1021/acs.jpcc.7b11771

Rutha K, Hayesa M, Burch R, Tsubota S, Haruta M (2000) The effects of SO_2 on the oxidation of CO and propane on supported Pt and Au catalysts. Appl Catal B Environ 24:133–138. https://doi.org/10.1016/S0926-3373(99)00100-9

Ryou Y, Lee J, Lee H, Choung JW, Yoo S, Kim DH (2015) Roles of ZrO_2 in SO_2-poisoned Pd/(Ce-Zr)O_2 catalysts for CO oxidation. Catal Today 258:518–524. https://doi.org/10.1016/j.cattod.2015.02.009

Saavedra J, Pursell CJ, Chandler BD (2018) CO oxidation kinetics over Au/TiO_2 and Au/Al_2O_3 catalysts: evidence for a common water-assisted mechanism. J Am Chem Soc 140:3712–3723. https://doi.org/10.1021/jacs.7b12758

Satsuma A, Yanagihara M, Ohyama J, Shimizu K (2013) Oxidation of CO over Ru/Ceria prepared by self-dispersion of Ru metal powder into nano-sized particle. Catal Today 201:62–67. https://doi.org/10.1016/j.cattod.2012.03.048

Schlexer P, Widmann D, Behm RJ, Pacchioni G (2018) CO oxidation on a Au/TiO_2 nanoparticle catalyst via the Au-assisted Mars–van Krevelen mechanism. ACS Catal 8:6513–6525. https://doi.org/10.1021/acscatal.8b01751

Schubert MM, Hackenberg S, van Veen AC, Muhler M, Plzak V, Behm RJ (2001) CO oxidation over supported gold catalysts—"inert" and "active" support materials and their role for the oxygen supply during reaction. J Catal 197:113–122. https://doi.org/10.1006/jcat.2000.3069

Shi JL, Zhao XJ, Zhang LY, Xue XL, Guo ZX, Gao YF, Li SF (2017) An oxidized magnetic Au single atom on doped TiO_2(110) becomes a high performance CO oxidation catalyst due to the charge effect. J Mater Chem A 5:19316–19322. https://doi.org/10.1039/c7ta05483a

Shin H, BaekM RY, Song C, Lee KY, Song IK (2018) Improvement of sulfur resistance of Pd/Ce–Zr–Al–O catalysts for CO oxidation. Appl Surf Sci 429:102–107. https://doi.org/10.1016/j.apsusc.2017.05.198

Smirnov MY, Kalinkin AV, Pashis AV, Prosvirin IP, Bukhtiyarov VI (2014) Interaction of SO_2 with Pt model supported catalysts studied by XPS. J Phys Chem C 118:22120–22135. https://doi.org/10.1021/jp5069126

Spezzati G, Benavidez AD, DeLaRiva AT, Su Y, Hofmann JP, Asahina S et al (2019) CO oxidation by Pd supported on CeO_2(100) and CeO_2(111) facets. Appl Catal B Environ 243:36–46. https://doi.org/10.1016/j.apcatb.2018.10.015

Taira K, Einaga H (2019) The effect of SO_2 and H_2O on the interaction between Pt and TiO_2(P-25) during catalytic CO oxidation. Catal Lett 149:965–973. https://doi.org/10.1007/s10562-019-02672-3

Taira K, Nakao K, Suzuki K, Einaga H (2016) SO_x tolerant Pt/TiO_2 catalysts for CO oxidation and the effect of TiO_2 supports on catalytic activity. Environ Sci Technol 50:9773–9780. https://doi.org/10.1021/acs.est.6b01652

Tanaka KI, He H, Yuan Y (2015) Catalytic oxidation of CO on metals involving an ionic process in the presence of H_2O: the role of promoting materials. RSC Adv 5:949–959. https://doi.org/10.1039/C4RA08349K

Tomita A, Shimizu KI, Kato K, Akita T, Tai Y (2013) Mechanism of low-temperature CO oxidation on Pt/Fe-containing alumina catalysts pretreated with water. J Phys Chem C 117:1268–1277. https://doi.org/10.1021/jp304940f

Valechha D, Megarajan SK, Fakeeha AH, Al-Fatesh AS, Labhasetwar NK (2017) Effect of SO_2 on catalytic CO oxidation over nano-structured, mesoporous Au/$Ce_{1-x}Zr_xO_2$ catalysts. Catal Lett 147:2893–2900. https://doi.org/10.1007/s10562-017-2182-6

Wakita H, Kani Y, Ukai K, Tomizawa T, Takeguchi T, Ueda W (2005) Effect of SO_2 and H_2S on CO preferential oxidation in H_2-rich gas over Ru/Al_2O_3 and Pt/Al_2O_3 catalysts. Appl Catal A Gen 283:53–61. https://doi.org/10.1016/j.apcata.2004.12.035

Wang J, Wang Z, Liu CJ (2014) Enhanced activity for CO oxidation over WO_3 nanolamella supported Pt catalyst. ACS Appl Mater Interfaces 6:12860–12867. https://doi.org/10.1021/am502807b

Wang C, Sasmaz E, Wen C, Lauterbach J (2015) Pd supported on SnO_2–MnO–CeO_2 catalysts for low temperature CO oxidation. Catal Today 258:481–486. https://doi.org/10.1016/j.cattod.2015.02.01

Wang C, Gu XK, Yan H, Lin Y, Li J, Liu D, Li WX, Lu J (2016) Water-mediated Mars–Van Krevelen mechanism for CO oxidation on ceria-supported single-atom Pt_1 catalyst. ACS Catal 7:887–891. https://doi.org/10.1021/acscatal.6b02685

Wang L, Pu C, Xu L, Cai Y, Guo Y, Guo Y et al (2017a) Effect of supports over Pd/Fe_2O_3 on CO oxidation at low temperature. Fuel Process Technol 160:152–157. https://doi.org/10.1016/j.fuproc.2017.02.037

Wang C, Wen C, Lauterbach J, Sasmaz E (2017b) Superior oxygen transfer ability of Pd/MnO_x-CeO_2 for enhanced low temperature CO oxidation activity. Appl Catal B Environ 206:1–8. https://doi.org/10.1016/j.apcatb.2017.01.020

Wang T, Xing JY, Zhu L, Jia AP, Wang YJ, Lu JQ, Luo MF (2019) CO oxidation over supported Pt/$Cr_xFe_{2-x}O_3$ catalysts and their good tolerance to CO_2 and H_2O. Appl Catal B Environ 245:314–324. https://doi.org/10.1016/j.apcatb.2018.12.054

Wang T, Xing JY, Jia AP, Tang C, Wang YJ, Luo MF, Lu JQ (2020) CO oxidation over Pt/$Cr_{1.3}Fe_{0.7}O_3$ catalysts: enhanced activity on single Pt atom by H_2O promotion. J Catal 382:192–203. https://doi.org/10.1016/j.jcat.2019.12.033

Wei S, Fu XP, Wang WW, Jin Z, Song QS, Jia CJ (2018) Au/TiO_2 catalysts for CO oxidation: effect of gold state to reactivity. J Phys Chem C 122:4928–4936. https://doi.org/10.1021/acs.jpcc.7b12418

Widmann D, Behm RJ (2013) Activation of molecular oxygen and the nature of the active oxygen species for CO oxidation on oxide supported Au catalysts. Acc Chem Res 47:740–749. https://doi.org/10.1021/ar400203e

Wu Z, Zhou SH, Zhu HG, Dai S, Overbury SH (2009) DRIFTS-QMS study of room temperature CO oxidation on Au/SiO_2 catalyst: nature and role of different Au species. J Phys Chem C 113:3726–3734. https://doi.org/10.1021/jp809220z

Xu J, White T, Li P, He CH, Yu JG, Yuan WK (2010) Biphasic Pd-Au alloy catalyst for low-temperature CO oxidation. J Am Chem Soc 132:10398–10406. https://doi.org/10.1021/ja102617r

Xu J, Zhang J, Peng H, Xu X, Liu W, Wang Z, Zhang N, Wang X (2017) Ag supported on meso-structured SiO_2 with different morphologies for CO oxidation: on the inherent factors influencing the activity of Ag catalysts. Microporous Mesoporous Mater 242:90–98. https://doi.org/10.1016/j.micromeso.2017.01.016

Xu ZC, Li YR, Lin YT, Zhu TY (2020) A review of the catalysts used in the reduction of NO by CO for gas purification. Environ Sci Pollut Res 27:6723–6748. https://doi.org/10.1007/s11356-019-07469-w

Yang Q, Du L, Wang X, Jia C, Si R (2016) CO oxidation over Au/ZrLa-doped CeO_2 catalysts: synergistic effect of zirconium and lanthanum. Chin J Catal 37:1331–1339. https://doi.org/10.1016/S1872-2067(15)61113-5

Yao Q, Wang C, Wang H, Yan H, Lu J (2016) Revisiting the Au particle size effect on TiO_2-coated Au/TiO_2 catalysts in CO oxidation

reaction. J Phys Chem C 120:9174–9183. https://doi.org/10.1021/acs.jpcc.5b12712

Yu F, Qu Z, Zhang X, Fu Q, Wang Y (2013) Investigation of CO and formaldehyde oxidation over mesoporous Ag/Co_3O_4 catalysts. J Energy Chem 22:845–852. https://doi.org/10.1016/S2095-4956(14)60263-1

Zhai X, Liu C, Chang Q, Zhao C, Tan R, Peng H, Liu D, Zhang P, Gui J (2018) TiO_2-nanosheet-assembled microspheres as Pd-catalyst support for highly-stable low-temperature CO oxidation. New J Chem 42:18066–18076. https://doi.org/10.1039/C8NJ03768J

Zhang Y, Wu Y, Wang H, Guo Y, Wang L, Zhan W, Guo Y, Lu G (2015) The effects of the presence of metal Fe in the CO oxidation over Ir/FeO_x catalyst. Catal Commun 61:83–87. https://doi.org/10.1016/j.catcom.2014.12.018

Zhang X, Dong H, Wang Y, Liu N, Zuo Y, Cui L (2016a) Study of catalytic activity at the Ag/Al-SBA-15 catalysts for CO oxidation and selective CO oxidation. Chem Eng J 283:1097–1107. https://doi.org/10.1016/j.cej.2015.08.064

Zhang X, Dong H, Zhao D, Wang Y, Wang Y, Cui L (2016b) Effect of support calcination temperature on Ag structure and catalytic activity for CO oxidation. Chem Res Chin U 32:455–460. https://doi.org/10.1007/s40242-016-5377-2

Zhang X, Cheng S, Zhang W, Zhang C, Drewett NE, Wang X, Wang D, Yoo SJ, Kim JG, Zheng W (2017) Mechanistic insight into nanoarchitected Ag/Pr_6O_{11} catalysts for efficient CO oxidation. Ind Eng Chem Res 56:11042–11048. https://doi.org/10.1021/acs.iecr.7b02530

Zhang X, Yang Y, Song L, Wang Y, He C, Wang Z, Cui L (2018) High and stable catalytic activity of Ag/Fe_2O_3 catalysts derived from MOFs for CO oxidation. Mol Catal 447:80–89. https://doi.org/10.1016/j.mcat.2018.01.007

Zhang N, Li L, Wu R, Song L, Zheng L, Zhang G, He H (2019a) Activity enhancement of Pt/MnO_x catalyst by novel β-MnO_2 for low-temperature CO oxidation: study of the $CO–O_2$ competitive adsorption and active oxygen species. Catal Sci Technol 9:347–354. https://doi.org/10.1039/C8CY01879K

Zhang LL, Sun MJ, Liu CG (2019b) CO oxidation on the phosphotungstic acid supported Rh single–atom catalysts via Rh–assisted Mans–van Krevelen mechanism. Mol Catal 462:37–45. https://doi.org/10.1016/j.mcat.2018.10.017

Zhao X, Hu Y, Jiang H, Yu J, Jiang R, Li C (2018) Engineering TiO_2 supported Pt sub-nanoclusters via introducing variable valence Co ion in high-temperature flame for CO oxidation. Nanoscale. 10:13384–13392. https://doi.org/10.1039/C7NR08717A

Zhao S, Chen F, Duan S, Shao B, Li T, Tang H, Lin Q, Zhang J, Li L, Huang J, Bion N, Liu W, Sun H, Wang AQ, Haruta M, Qiao B, Li J, Liu J, Zhang T (2019) Remarkable active-site dependent H_2O promoting effect in CO oxidation. Nat Commun 10:3824. https://doi.org/10.1038/s41467-019-11871-w

Zheng B, Wu S, Yang X, Jia M, Zhang W, Liu G (2016) Room temperature CO oxidation over $Pt/MgFe_2O_4$: a stable inverse spinel oxide support for preparing highly efficient Pt catalyst. ACS Appl Mater Interfaces 8:26683–26689. https://doi.org/10.1021/acsami.6b06501

Zhou Y, Wang Z, Liu C (2015) Perspective on CO oxidation over Pd-based catalysts. Catal Sci Technol 5:69–81. https://doi.org/10.1039/C4CY00983E

Zhou Y, Doronkin DE, Chen M, Wei S, Grunwaldt JD (2016) Interplay of Pt and crystal facets of TiO_2: CO oxidation activity and operando XAS/DRIFTS studies. ACS Catal 6:7799–7809. https://doi.org/10.1021/acscatal.6b01509

Zorn K, Giorgio S, Halwax E, Henry CR (2011) CO oxidation on technological $Pd–Al_2O_3$ catalysts: oxidation state and activity. J Phys Chem C 115:1103–1111. https://doi.org/10.1021/jp106235x